OPEN ACCESS

African Journal of Environmental Science and Technology

September 2023
ISSN 1996-0786
DOI: 10.5897/AJEST
www.academicjournals.org

ACADEMIC JOURNALS
expand your knowledge

About AJEST

African Journal of Environmental Science and Technology (AJEST) provides rapid publication (monthly) of articles in all areas of the subject such as Biocidal activity of selected plant powders, evaluation of biomass gasifier, green energy, Food technology etc. The Journal welcomes the submission of manuscripts that meet the general criteria of significance and scientific excellence. Papers will be published shortly after acceptance. All articles are peer-reviewed

Indexing

The African Journal of Environmental Science and Technology is indexed in:
CAB Abstracts, CABI's Global Health Database, Chemical Abstracts (CAS Source Index), China National Knowledge Infrastructure (CNKI), Dimensions Database, Google Scholar, Matrix of Information for The Analysis of Journals (MIAR), Microsoft Academic

AJEST has an h5-index of 14 on Google Scholar Metrics

Open Access Policy

Open Access is a publication model that enables the dissemination of research articles to the global community without restriction through the internet. All articles published under open access can be accessed by anyone with internet connection.

The African Journal of Environmental Science and Technology is an Open Access journal. Abstracts and full texts of all articles published in this journal are freely accessible to everyone immediately after publication without any form of restriction.

Article License

All articles published by African Journal of Environmental Science and Technology are licensed under the Creative Commons Attribution 4.0 International License. This permits anyone to copy, redistribute, remix, transmit and adapt the work provided the original work and source is appropriately cited. Citation should include the article DOI. The article license is displayed on the abstract page the following statement:

This article is published under the terms of the Creative Commons Attribution License 4.0
Please refer to https://creativecommons.org/licenses/by/4.0/legalcode for details about Creative Commons Attribution License 4.0

Memberships and Standards

Academic Journals strongly supports the Open Access initiative. Abstracts and full texts of all articles published by Academic Journals are freely accessible to everyone immediately after publication.

Crossref is an association of scholarly publishers that developed Digital Object Identification (DOI) system for the unique identification published materials. Academic Journals is a member of Crossref and uses the DOI system. All articles published by Academic Journals are issued DOI.

Similarity Check powered by iThenticate is an initiative started by CrossRef to help its members actively engage in efforts to prevent scholarly and professional plagiarism. Academic Journals is a member of Similarity Check.

CrossRef Cited-by Linking (formerly Forward Linking) is a service that allows you to discover how your publications are being cited and to incorporate that information into your online publication platform. Academic Journals is a member of CrossRef Cited-by.

Academic Journals is a member of the International Digital Publishing Forum (IDPF). The IDPF is the global trade and standards organization dedicated to the development and promotion of electronic publishing and content consumption.

Contact

Editorial Office: ajest@academicjournals.org

Help Desk: helpdesk@academicjournals.org

Website: http://www.academicjournals.org/journal/AJEST

Submit manuscript online http://ms.academicjournals.org

Academic Journals
73023 Victoria Island, Lagos, Nigeria
ICEA Building, 17th Floor,
Kenyatta Avenue, Nairobi, Kenya.

Table of Content

Vol. 17(9), pp. 209-218, September 2023
DOI: 10.5897/AJEST2022.3157
Article Number: 06502A171191
ISSN: 1996-0786

http://www.academicjournals.org/AJEST

African Journal of Environmental Science and Technology

Full Length Research Paper

Degradation of chlorantraniliprole by photocatalysis of supported titanium dioxide: Effect of operating parameters

N'GUETTIA Kossonou Roland[1]*, DIARRA Moussa[2], SORO Baba Donafologo[1], ABOUA Kouassi Narcisse[1], GOMBERT Bertrand[3] and TRAORE Karim Sory[1]

[1]Environmental Sciences Laboratory, Nangui Abrogoua University, 02 BP 801 Abidjan 02, Ivory Coast.
[2]Environmental Sciences and Technologies Laboratory (LSTE), Jean Lorougnon GUEDE University, Ivory Coast.
[3]Institute of Chemistry of Environments and Materials of Poitiers (IC2MP), University of Poitiers, France.

Received 19 September, 2022; Accepted 20 December, 2022

The rinsing of sprayers after the phytosanitary treatment of agricultural plots generates waste water, which is discharged without prior treatment into aquatic environments. The aim of this study was to evaluate the efficiency of a supported photocatalytic process for the degradation of chlorantraniliprole in an aqueous medium. Clay balls were made in the laboratory from 40 mL of ultrapure water added to 100 g of clay powder to obtain a homogeneous paste. Beads were made and dried at 105°C for 24 h and then baked at 550°C in the oven to make them water-resistant. They were soaked in a 10 g/L ethanol solution of TiO_2 for 24 h, then calcined at 400°C. The photocatalysis experiments were carried out with 50 ml reactors containing 40 g of beads under sunlight in a humid tropical zone for 300 min. The results showed a decrease in the concentration of chlorantraniliprole 500 µg/L under theses experimental conditions. The degradation of this insecticide is significantly improved by increasing the clay mass at pH = 6 for a concentration of 500 µg/L. In addition, the application of this photocatalytic process on environmental matrices showed that this process was effective for the depollution of drinking water and river water. The beads were reused for all experiments by recycling them by calcination at 400°C.

Key words: Chlorantraniliprole, supported titanium dioxide, clay beads, aqueous medium.

INTRODUCTION

Although there are many new methods of insect control, chemical control using insecticides has long been considered a reliable method (Hafeez et al., 2019). For example, plant protection products are specifically designed to elicit a biological response in a specific organism (Li et al., 2022). However, some can also elicit the same response in nonspecific creatures following persistent exposure to even minute amounts of these chemicals (Héma et al., 2009; Khan et al., 2022). As part of the search for alternative molecules to pyrethroids that are effective against insect pests of cotton in the Sahelian zone, chlorantraniliprole, which belongs to the anthranilic diamide family, was authorized in 2014 under the brand name CORAGEN 20 SC. It has been successfully tested at research stations and on growers' farms (Cordova et al., 2006; Lahm et al., 2007). However, despite the good

*Corresponding author. E-mail: rolandkossonou@yahoo.fr. Tel. (00243)89 46 99 243.

quality of the results obtained on cotton plots, the management of sprayer rinse water near water resources located in the drinking water resources of the major cities of Côte d'Ivoire is becoming a problem in agricultural areas. Indeed, due to their high leachability and with a leaching potential index of 4.22 (Lewis and Tzilivakis, 2017; Fenoll et al., 2015), chlorantraniliprole and some of its metabolites can leach through the soil profile. In addition, chlorantraniliprole is considered persistent and mobile in surface waters and exhibits relatively high aquatic toxicity (Aliste et al., 2021). Photocatalytic degradation has been considered an effective and inexpensive tool for the removal of organic and inorganic pollutants from water (Rodrigues-Silva et al., 2013; Chong et al., 2010). Many studies have used an aqueous suspension of anatase (TiO_2) in different physico-chemical forms, to degrade pollutants by UV illumination (Prieto-Rodríguez et al,. 2013). The most commonly commercially available powder form of TiO_2, shows significant photocatalytic activity (Koltsakidou et al., 2017). However, due to its nanometric size, its use requires an additional and somewhat difficult operation to separate it from treated water. Extensive research has been reported for the immobilization of TiO_2 on a photo-chemically stable substrate such as clay minerals (Heidari et al., 2022). The present study aims to develop a solid support (clay) easily available, recyclable, reusable and ecological to immobilize TiO_2 for the application in the processes of photocatalytic degradation of chlorantraniliprole in aqueous medium. Specifically, it will involve determining the kinetics of chlorantraniliprole degradation and highlighting the influence of certain parameters such as the initial concentration of the pollutant, the initial mass of the catalyst, the pH and the dilution matrices on the kinetics of photocatalytic degradation.

MATERIALS AND METHODS

Chemical products

The quality of the products used is of purity greater than 95%. Carlos Erba brand analysis grade ethanol and acetone were 99.99% pure. HPLC grade acetonitrile is of 99.99% purity. The chlorantraniliprole used is a phytosanitary product called CORAGEN 20 SC with a concentration of 200 g/L. The oxidant is titanium dioxide (TiO_2) composed of anatase of 99% purity. It was supplied by the firm Carlos Erba.

Protocol for the production of clay balls

For the production of clay balls with or without TiO_2, two protocols were carried out in each case: calcined pure clay balls were made and the fixing of TiO_2 on the calcined balls.

Making calcined balls

To make calcined clay beads, 40 mL of ultrapure water were added to 100 g of clay powder to obtain a homogeneous paste (Step 1). Beads of about 0.3 mm in diameter were made. These balls were then dried at 105°C (Step 2) for 24 h and then baked at 550°C in the oven to make them resistant in water (Step 3) and also to eliminate all forms of residual organic matter (Figure 1).

Beads covered of TiO_2 making

The clay beads were soaked in an ethanolic solution of 20 g/L of TiO_2 for three days. Then, the beads were calcined in the oven at 400°C for 2 h on a temperature ramp of 10°C/min. This ramp promotes fixation of a large quantity of TiO_2. The beads were rinsed with ultrapure water to get rid of the TiO_2 residues which were not well fixed. This experiment was repeated three times to allow better fixation of the TiO_2 (Figure 2).

Clay beads characterization tests

Analysis by scanning electron microscopy

Scanning electron microscopy (SEM) is a surface characterization technique allowing observations down to the nanometric scale. Before being observed in the SEM, a gold/palladium (Au/Pd) deposit is made on the samples. This metallization avoids the accumulation of charge on the surface of the sample and decreases the penetration depth of the beam, thus improving the quality of the image. The SEM observations were carried out on a Philips XL 30 device at 15 kV coupled to an EDX (Energy Dispersive Xray) microanalysis.

X-ray microanalysis analysis

Energy dispersive X-ray microanalysis, EDX, with a scanning electron microscope allows qualitative and quantitative analyses of small sample volumes of beads coated or not with TiO_2. Qualitative X-ray microanalysis is performed using energy dispersive element spectra.

Experiments

Adsorption test

Adsorption experiments were carried out in the dark both with the beads covered with TiO_2 and with those not covered with TiO_2. The duration of the test is 300 min.

Photolysis test

The photolysis consisted in the irradiation of the doped matrices at concentrations of 500 µg/L under solar irradiation in the presence of beads not covered with TiO_2. The objective is to know the contribution of direct photolysis during the degradation of the chlorantraniliprole. Samples were then taken successively with Pasteur pipettes at regular time intervals during irradiation (30, 60, 120, 180, 240, and 300 min) and analyzed by high performance liquid chromatograph coupled to a UV detector.

Experimental photocatalytic

The experimental device is composed of four 50 mL test tubes corresponding to the different times of the experiments. The water matrices were spiked with the chlorantraniliprole solutions. The

Figure 1. Steps in the manufacture of calcined clay beads.
Source: Authors

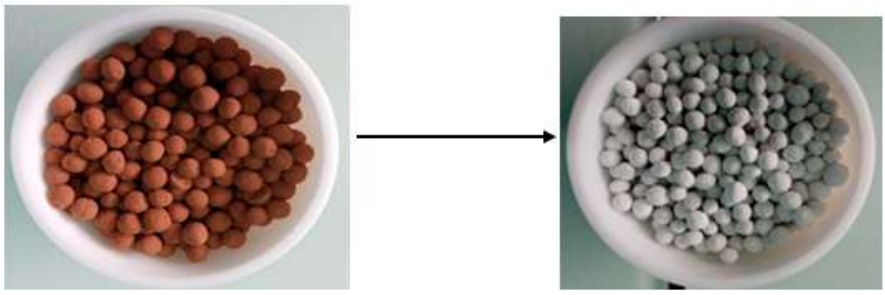

Figure 2. Steps in the manufacture of clay balls covered with titanium dioxide.
Source: Authors

reactors were placed under natural solar radiation. The duration of each test is 300 min. Samples are then taken successively with Pasteur pipettes at regular time intervals during the irradiation (30, 60, 120, 180, 240, and 300 min) and analyzed by high performance liquid chromatograph. After each photocatalysis test, the reactors and the clay balls were calcined in an oven at 400°C for 2 h to destroy the pesticide residues. The effect of parameters such as the mass of beads impregnated in TiO_2, the concentration of the pollutant, the pH and the dilution matrices was studied under these studies conditions.

Photodegradation kinetics

When photolysis or photocatalysis is used for the removal of organic pollutants in aqueous media, the degradation kinetics conforms to the Langmuir-Hinshelwood model. These kinetics describe the reactions between the $OH^{\bullet}$ radicals and the adsorbed or dissolved organic molecules. This model is generally first-order kinetics. This reaction is described by Equations 1 to 3.

$$\frac{dc}{dt} = k_{app} \times t \quad (1)$$

$$\ln\left(\frac{C_0}{C}\right) = k_{app} \times t \quad (2)$$

$$t_{1/2} = \frac{\ln 2}{k} \quad (3)$$

k_{app} is pseudo order 1 kinetic constant; $t_{1/2}$: reaction half-life time

RESULTS AND DISCUSSION

SEM-EDX scanning electron microscopy

SEM analysis of the various calcined balls is as shown in Figure 3a and b. The results indicate two different topographies of the surface of the two types of clay balls. Observation of the beads coated with TiO_2 show a white color characteristic of the presence of titanium dioxide in Figure 3.

X-ray diffraction of the different balls analysis

The elementary composition of the different calcined balls is as shown in Figure 4a and b. The results showed that seven (07) elements identified (O, Si, C, Ti, Al, P, Fe, S). Aluminium, silicon and oxygen are the main chemical elements in the calcined balls not covered with TiO_2. As for the clay, balls are covered with TiO_2, the results showed a decrease in the energies of the 7 chemical elements and a predominantly appearance of TiO_2. These results confirm those obtained by scanning electron microscopy.

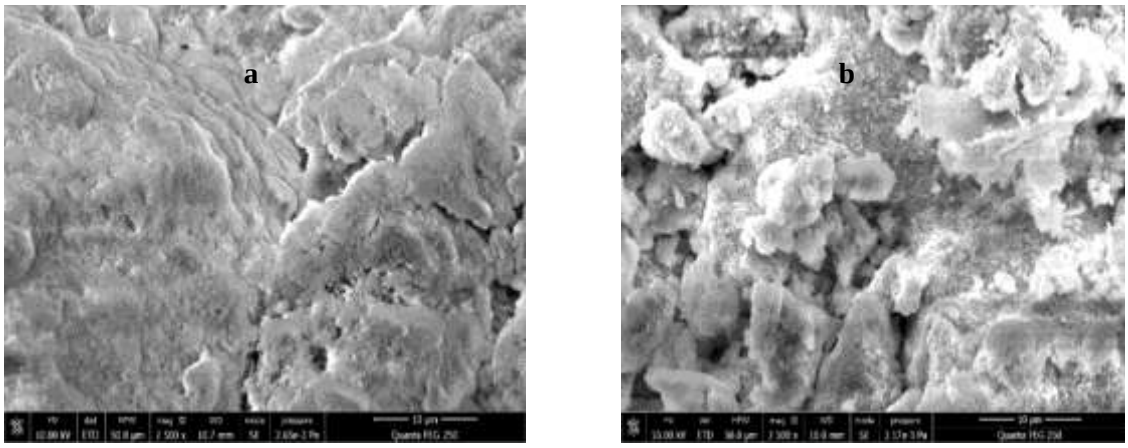

Figure 3. SEM images of calcined clay balls not covered with TiO_2 (a) and covered with TiO_2 (b).
Source: Authors

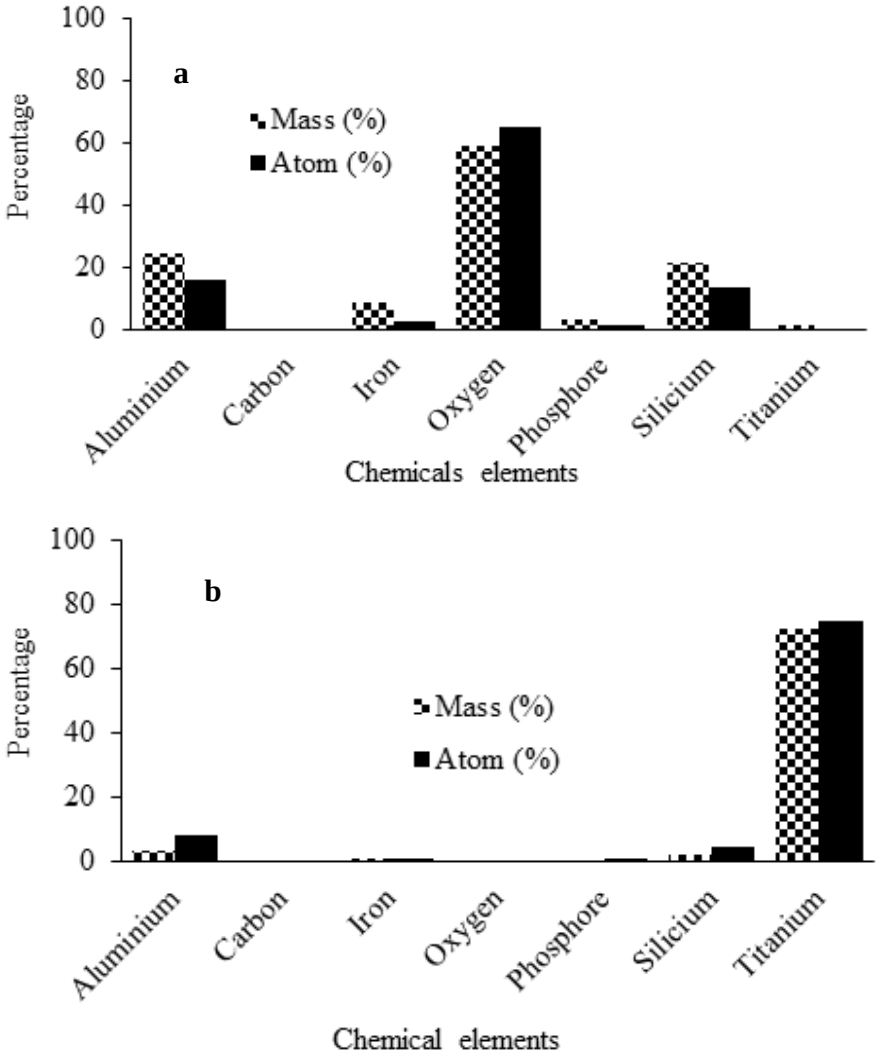

Figure 4. Elemental composition of calcined clay balls (a) not covered with TiO_2 and (b) covered with TiO_2.
Source: Authors

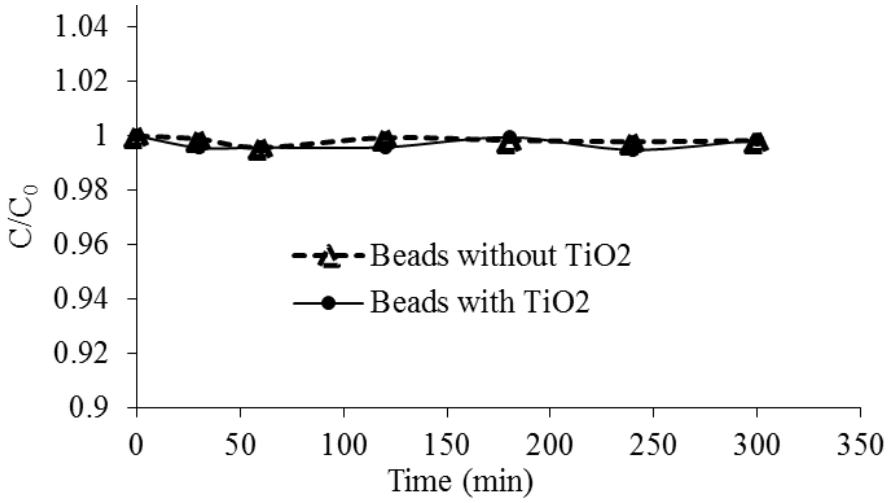

Figure 5. Adsorption tests in the presence of simple clays soaked in TiO_2, V = 50 mL, C_0 = 500 µg/l, T = 25°C, weight = 40 g; pH = 6 .
Source: Authors

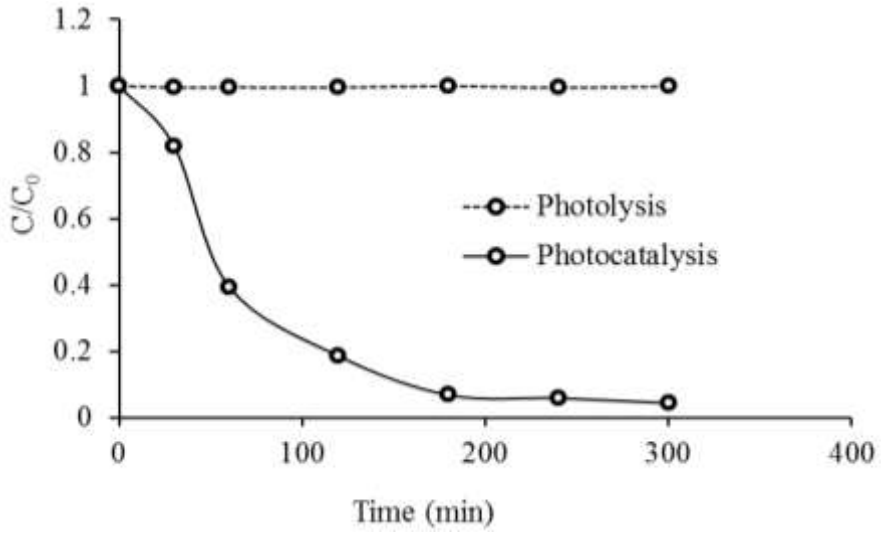

Figure 6. Kinetics of photolysis and solar photocatalysis of chlorantraniliprole, C_0 = 500 µg/L, clay weight = 40 g, V = 50 mL, pH = 6.
Source: Authors

Adsorption test

Absorption experiments were carried out on beads without TiO_2 and beads covered with TiO_2. Figure 5 shows the adsorption kinetics of chlorantraniliprole under our experimental conditions. The two adsorption tests were carried out to evaluate the adsorption capacity of the insecticide on the beads soaked in TiO_2 or not. For this, control clay balls and balls soaked in TiO_2 as adsorbent were used during these experiments. The results indicated chlorantraniliprole is not removed by adsorption tests. These results showed that chlorantraniliprole does not adsorb to the surface of clay materials.

Photodegradation tests

Direct photolysis and solar photocatalysis tests were carried out by exposing reactors to room temperature illustrated in Figure 6. The direct photolysis experiment by solar exposure indicated that the initial concentration

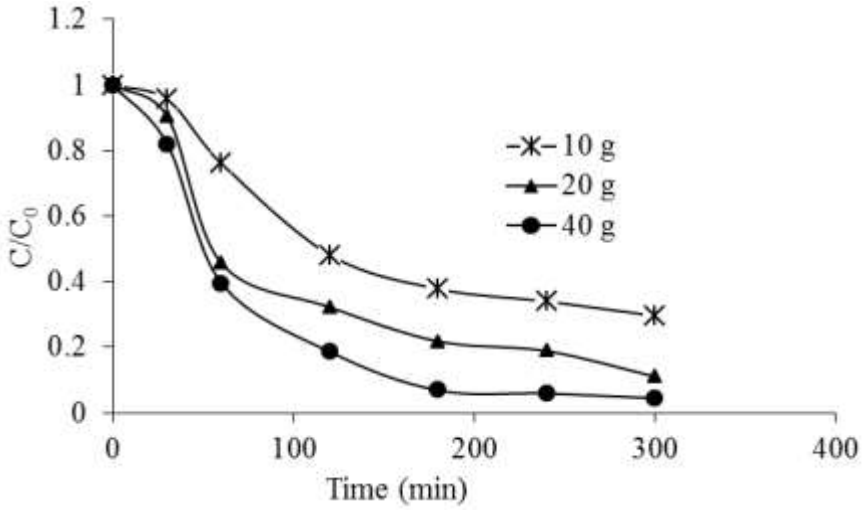

Figure 7. Effect of catalyst concentration, pH = 6, C_0 = 500 µg/L, T = 25°C.
Source: Authors

of PAC did not change. These results are in agreement with those obtained by Lin et al. (2017) . These authors have also shown that a pesticide cannot be degraded by direct photolysis under similar conditions since this anticancer molecule does not have chromophores which absorb UVA (N'guettia et al., 2017). Unlike photolysis, the solar photocatalysis experiment indicated a break in slope. This rupture is followed by a decrease in the initial concentration of chlorantraniliprole during the solar irradiation. This decrease in initial concentrations would reflect a photocatalytic oxidation of phytosanitary pollutants by $OH^{\bullet}$ radicals. Indeed, most of these processes combine two or three reagents (oxidants) to produce OH radicals$^{\bullet}$ (Fenoll et al., 2015; Gad-Allah et al., 2011). Free radicals are highly active species capable of reacting rapidly and non-selectively on most organic compounds, deemed to be difficult to oxidize biologically or by conventional chemical treatments (Simon et al., 2008; Magnone et al., 2019).

Effect of TiO_2 concentration

To study the effect of catalyst mass, we increased the mass of beads covered with TiO_2 from 10 to 40 g. Figure 7 shows the evolution of the disappearance of chlorantraniliprole for these different masses of the catalyst. The results showed that whatever the mass of balls coated with TiO_2, 50% of the concentration of the pollutant is degraded after 1 h of reaction. After 300 min of experiment, the rates of disappearance obtained from this insecticide were 70.40, 88.91, and 95.54%. The increase in the mass of the beads covered with the catalyst induces a strong disappearance of chlorantraniliprole in the doped solutions. However, the mass of beads coated with TiO_2 is not proportional to the rate of degradation obtained. This could result in a disparity of the TiO_2 fixed on the surface of the beads. The maximum speed is reached for a mass of 40 g of the TiO_2 catalyst. These results are similar to those of Xekoukoulotakis et al. (2011) and Michael et al. (2013). These authors have shown that this efficiency reflects an abundant production of hydroxyl radicals. This efficiency would be due to an increase in the exposed surface of the TiO_2 fixed on the clay beads.

Effect of pollutant concentration

Figure 8 shows the degradation kinetics of chlorantraniliprole in the different reactors. The degradation of the substrate is therefore inversely proportional to the initial concentration of the latter. This fact would be explained by a weaker participation of photons as the concentration of the solute increases; consequently a saturation of the sites of sites of the production of $OH^{\bullet}$ radicals. The reduction rates of the initial concentration of the pollutant are 95.54, 62.74, and 53.26%, respectively for the 500 concentrations; 1000 and 1500 µg/L of pollutant. This phenomenon can be explained by the reduction in the photodegradation of h^{+} holes and/or $OH^{\bullet}$ radicals on the surface of the catalyst due to the covering of the active sites by the pollutant, or by the reduction in intensity of the radiation absorbed at the level of the catalyst caused by the molecules of the pollutant (Simon et al., 2008).

Figure 9 shows the rate equations for the degradation of chlorantraniliprole at different concentrations. The expression of the equation $\ln\left(\frac{C_0}{C}\right) = kt$ is straight with

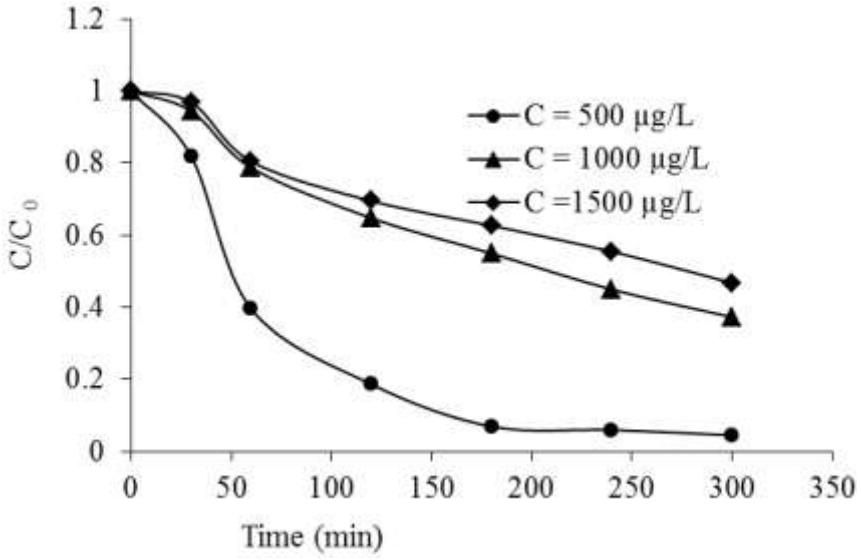

Figure 8. Effect of chlorantraniliprole concentration, weight of beads-TiO_2 = 40 g; T = 25°C, pH = 6.
Source: Authors

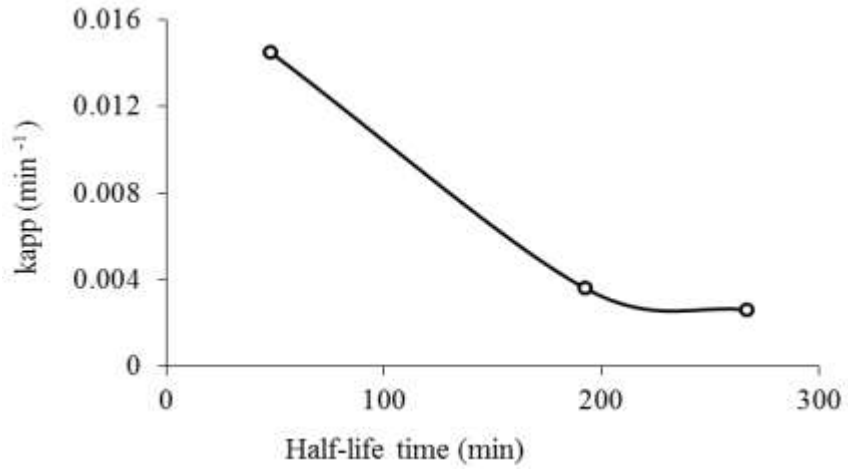

Figure 9. Right-hand equation as a function of irradiation time in ultrapure water.
Source: Authors

correlation coefficients R^2 equal to 0.99 for the different concentrations of pollutants. The disappearance kinetics of chlorantraniliprole follows a first-order law. The values of the kinetic constants are $2.6.10^{-3}$, $3.4.10^{-3}$ and $1.45.10^{-2}$ min^{-1}. The results indicated that the rate constant (k_{app}) decreases with increasing substrate concentration. And as a result, half-life times were reduced from 267 to 48 min for chlorantraniliprole concentrations of 500 to 1500 µg/L. In fact, in water, chlorantraniliprole is persistent under aerobic conditions with a half-life varying from 125 to 231 days (median of 178 days). It is moderately persistent under anaerobic conditions (half-life = 42 days) at 25°C. In addition, metabolites such as (2-[3-bromo-1-(3-chloro-2-pyridinyl)-1H-pyrazol-5-yl]-6-chloro-3,8 dimethyl-4(3H)-quinazolinone, is also persistent in aerobic soils where its half-life ranges from 646 to 785 days. In water, this metabolite is persistent with half-lives of 121 to 680 days (aerobic) and 701 days (anaerobic).

Effect of pH

Figure 10 shows the degradation kinetics of chlorantraniliprole at different values of pH. The variation

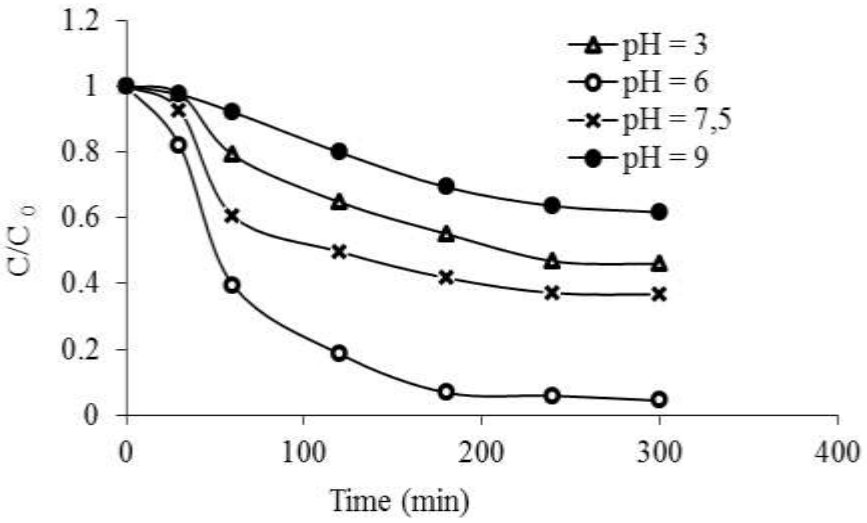

Figure 10. Degradation kinetics of chlorantraniliprole as a function of pH, C_0 = 500 µg/L, weight = 40 g.
Source: Authors

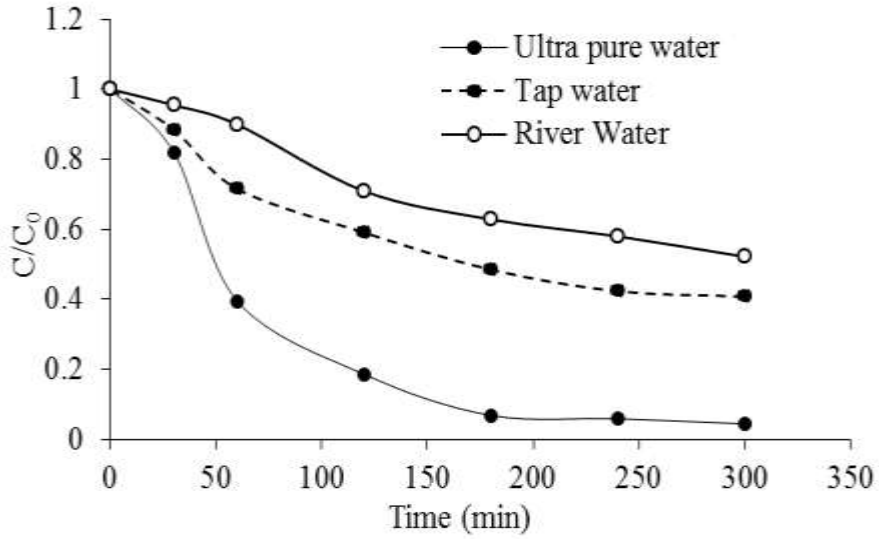

Figure 11. Degradation kinetics of chlorantraniliprole according to the dilution matrices, C_0 = 500 µg/L, weight = 40 g.
Source: Authors

of the pH makes it possible to highlight the ionic forms of the organic molecules in this study. Depending on the value of this pKa, we varied the pH values of the solutions to be irradiated from 3 to 9. In the case of chlorantraniliprole, the pKa value is 10. This shows that chlorantraniliprole would practically exist in its cationic form in aqueous environmental media. These results revealed that the cationic form of chlorantraniliprole is eliminated at different pH values of the spiked waters.

Effect of water matrices

The influence of environmental water matrices was studied. The aim is to optimize the removal process of chlorantraniliprole from ordinary waters. For this, drinking water or tap water was used in addition to ultra-pure water as shown in Figure 11. The results indicated a gradual disappearance of this molecule in tap water than in river water spiked at 500 µg/L. These results showed a

difference in the degradation rates of chlorantraniliprole in these matrices which would be linked to the chemical composition of the irradiated matrices. These results are in agreement with those of Pereira et al. (2013) and Sheng et al. (2013). These authors indicated that HCO_3^- /CO_3^{2-} ions which are abundant in tap water or organic matter present in river water can trap OH radicals or attach themselves to h^+ holes. Also, these effects are complex due to the ability of some of them to compete with organic compounds for oxidizing species (Calza et al., 2006) or to adsorb on the active surface sites of the catalyst depending on the ionic strength. These mechanisms can reduce the overall catalytic activity and therefore the rate of degradation of organic molecules (Dionysiou et al., 2000) .

Conclusion

Photocatalytic oxidation TiO_2 fixed on clay balls under artificial light offers an interesting alternative for the detoxification of water polluted by chlorantraniliprole. Increasing the mass of beads covered with TiO_2 improved the degradation rate of this insecticide in this study. On the other hand, the concentration of the pollutant should be optimized with the mass of balls covered with TiO_2. For this study, the optimal pH value is between 6 and 10. Under these conditions, this solar photocatalytic process could also be effective for the depollution of environmental matrices.

CONFLICT OF INTERESTS

The authors have not declared any conflict of interests.

REFERENCES

Aliste M, Garrido I, Pérez-Lucas G, Navarro S, Fenoll J (2021). Photocatalytic oxidation of chlorantraniliprole, imidacloprid, pirimicarb, thiamethoxam and their main photoreaction interMediates as impacted by water matrix composition under UVA-LED exposure. Catalysts 11(5):609.

Calza P, Sakkas VA, Medana C, Baiocchi C, Dimou A, Pelizzetti E, Albanis T (2006). Photocatalytic degradation study of diclofenac over aqueous TiO_2 suspensions. Applied Catalysis B: Environmental 67(3):197-205.

Chong MN, Jin B, Chow CW, Saint C (2010). Recent developments in photocatalytic water treatment technology: a review. Water Research 44(10):2997-3027.

Cordova D, Benner EA, Sacher MD, Rauh JJ, Sopa JS, Lahm GP, Selby TP, Stevenson TM, Flexner L, Gutteridge S (2006). Anthranilic diamides: a new class of insecticides with a novel mode of action, ryanodine receptor activation. Pesticide Biochemistry and Physiology 84(3):196-214.

Dionysiou DD, Suidan MT, Bekou E, Baudin I, Laîné JM (2000). Effect of ionic strength and hydrogen peroxide on the photocatalytic degradation of 4-chlorobenzoic acid in water. Applied Catalysis B: Environmental 26(3):153-171.

Fenoll J, Garrido I, Cava J, Hellín P, Flores P, Navarro S (2015). Photometabolic pathways of chlorantraniliprole in aqueous slurries containing binary and ternary oxides of Zn and Ti. Chemical Engineering Journal 264:720-727.

Gad-Allah TA, Ali ME, Badawy MI (2011). Photocatalytic oxidation of ciprofloxacin under simulated sunlight. Journal of Hazardous Materials 186(1):751-755.

Hafeez M, Liu S, Jan S, Gulzar A, Fernández-Grandon GM, Qasim M, Khan KA, Ali B, Kedir SJ, Fahad M, Wang M (2019). Enhanced effects of dietary tannic acid with chlorantraniliprole on life table parameters and nutritional physiology of Spodoptera exigua (Hübner). Pesticide Biochemistry and Physiology 155:108-118.

Heidari A, Shahbazi A, Aminabhavi TM, Barceló D, Rtimi S (2022). A systematic review of clay-based photocatalysts for emergent micropollutants removal and microbial inactivation from aqueous media: Status and limitations. Journal of Environmental Chemical Engineering 10(6):108813.

Héma O, Somé HN, Traoré O, Greenplate J, Abdennadher M (2009). Efficacy of transgenic cotton plant containing the Cry1Ac and Cry2Ab genes of Bacillus thuringiensis against Helicoverpa armigera and Syllepte derogata in cotton cultivation in Burkina Faso. Crop Protection 28(3):205-214.

Khan S, Naushad Mu, Govarthanan M, Iqbal J, Alfadul SM (2022). Emerging contaminants of high concern for the environment: Current trends and future research. Environmental Research 207:112609.

Koltsakidou A, Antonopoulou M, Evgenidou E, Konstantinou I, Giannakas AE, Papadaki M, Bikiaris D, Lambropoulou DA (2017). Photocatalytical removal of fluorouracil using TiO_2-P25 and N/S doped TiO_2 catalysts: A kinetic and mechanistic study. Science of The Total Environment 578:257-267.

Lahm GP, Stevenson TM, Selby TP, Freudenberger JH, Cordova D, Flexner L, Bellin CA, Dubas CM, Smith BK, Hughes KA (2007). Rynaxypyr™: a new insecticidal anthranilic diamide that acts as a potent and selective ryanodine receptor activator. Bioorganic and Medicinal Chemistry Letters 17(22):6274-6279.

Lewis K, Tzilivakis J (2017). Development of a data set of pesticide dissipation rates in/on various plant matrices for the Pesticide Properties Database (PPDB). Data 2(3):28.

Li M, Gong C, Zhang Y, Zhao X, Jia Y, Pu J, Liu X, Xu X, Wang X (2022). Differences in susceptibility to chlorantraniliprole between Chilo suppressalis (Lepidoptera: Crambidae) and two dominant parasitic wasps collected from Sichuan Province, China. Pesticide Biochemistry and Physiology 185:105-150.

Lin L, Wang H, Xu P (2017). Immobilized TiO_2-reduced graphene oxide nanocomposites on optical fibers as high performance photocatalysts for degradation of pharmaceuticals. Chemical Engineering Journal 310:2:389-398.

Magnone E, Kim M-K, Lee HJ, Park JH (2019). Testing and substantial improvement of TiO_2/UV photocatalysts in the degradation of Methylene Blue. Ceramics international 45(3):3359-3367.

Michael I, Hapeshi E, Aceña J, Perez S, Petrović M, Zapata A, Barceló D, Malato S, Fatta-Kassinos D (2013). Light-induced catalytic transformation of ofloxacin by solar Fenton in various water matrices at a pilot plant: Mineralization and characterization of major intermediate products. Science of the Total Environment 461:39-48.

N'guettia RK, Gombert B, Soro B-D, Traore SK, Karpel NVL (2017). Dégradation photocatalytique du 5-fluorouracile par un système UV-A/TiO_2: effet de la concentration du catalyseur et du polluant, du pH et des matrices de dilution. International Journal of Biological and Chemical Sciences 11(3):1373-1385.

Pereira JHOS, Reis AC, Queirós D, Nunes OC, Borges MT, Vilar VJP, Boaventura RAR (2013). Insights into solar TiO2-assisted photocatalytic oxidation of two antibiotics employed in aquatic animal production, oxolinic acid and oxytetracycline. Science of the Total Environment 463-464:274-283.

Prieto-Rodríguez L, Oller I, Klamerth N, Agüera A, Rodríguez EM, Malato S (2013). Application of solar AOPs and ozonation for elimination of micropollutants in municipal wastewater treatment plant effluents. Water Research 47(4):1521-1528.

Rodrigues-Silva C, Maniero MG, Rath S, Guimarães JR (2013). Degradation of flumequine by photocatalysis and evaluation of antimicrobial activity. Chemical Engineering Journal 224:46-52.

Sheng H, Li Q, Ma W, Ji H, Chen C, Zhao J (2013). Photocatalytic degradation of organic pollutants on surface anionized TiO_2: Common effect of anions for high hole-availability by water. Applied

Catalysis B: Environmental 138:212-218.
Simon JC, Dauby B, Nonet S (2008). Evaluation de l'efficacité de l'oxydation avancée par photocatalyse hétérogène UV/TiO_2 sur un effluent industriel contaminé par des composés organiques non biodégradables (colorants). Revue scientifique des ISIL*F* 22:18-20.
Xekoukoulotakis NP, Drosou C, Brebou C, Chatzisymeon E, Hapeshi E, Fatta-Kassinos D, Mantzavinos D (2011). Kinetics of UV-A/TiO_2 photocatalytic degradation and mineralization of the antibiotic sulfamethoxazole in aqueous matrices. Catalysis Today 161(1):163-168.

Vol. 17(9), pp. 219-244, September 2023
DOI: 10.5897/AJEST2023.3177
Article Number: EC67A8D71193
ISSN: 1996-0786

http://www.academicjournals.org/AJEST

ACADEMIC JOURNALS
expand your knowledge

African Journal of Environmental Science and Technology

Full Length Research Paper

Water exploitation-induced climate change

Miah Muhammad Adel

Department of Physics, University of Arkansas, Pine Bluff, Pine Bluff, AR 71601, Arkansas, Humane Water, P. O. Box 782916, Wichita, KS, US.

Received 15 January, 2023; Accepted 19 June, 2023

Downstream countries can experience a range of direct, indirect, and feedback effects from upstream water piracy. These consequences can range from economic decline due to decreased availability of water for agriculture and fisheries, to the disruption of ecosystems from alterations to water flows and ecosystems, to the potential for political tensions that arise due to unequal access to water resources. The upstream country backs the downstream country's government to serve its own interests. The loss of the heat-storing water medium of the Aral Sea due to the former Soviet Union pirating water from the basin's feeding rivers for cotton production has resulted in warmer summers and cooler winters in the region than before. India is turning the basins of the Ganges and the Teesta into another Aral Sea basin, while deluging the basins with recurrent floods through the sudden release of water from the Farakka and Teesta barrages, and other trans-border river barrages. India's threat to revoke the more than six-decade-old Indus River water treaty has put Pakistan at a severe disadvantage, as extreme climatic events and an increase in irrigation progression have been linked to an increase in lightning-related fatalities. Some Nobel Laureate Professors have mistakenly identified energy insolvency as the cause of water piracy amid the competing plans of building dams and barrages by India and China, which threatens to turn the lower Brahmaputra and Mekong basins into another Aral Sea-like disaster Climatologists should soon embark on a holistic study of CO_2 emissions and surface water exploitation in order to keep the planet livable, and use water for necessity rather than greed.

Key words: Water piracy, Aral Sea, Ganges, Teesta, Brahmaputra, Indus, Mekong, Indus water treaty, CO_2, Bangladesh, Farakka Barrage, Teesta Barrage, dams, barrages.

INTRODUCTION

The article covers Asian countries affected by the upstream water piracy. Figure 1 shows regions where these countries-Kazakhstan, Uzbekistan, Pakistan, India, Bangladesh, China, Cambodia, Laos, Myanmar, Peninsular Malaysia, Thailand, and Vietnam – are located. Guided by the idea of being rich in a shorter time, the former USSR first started this antienvironmental activity of pirating water from the Amu Darya and the Sir Darya (Figure 2), the head streams of the world's 4th largest inland water source the Aral Sea (45.3963° N, 59.6134° E) (Figure 3, http://www.columbia.edu/~tmt2120/environmental%20impacts.htm; Figures 4 and 5, https://openoregon.pressbooks.pub/envirobiology/chapter/7-5-case-study-the-aral-sea-going-going-gone/). Being

E-mail: adelm@uapb.edu.

Figure 1. An atlas of Asia the extreme weather like summertime.
Source: Anthony (2006).

Figure 2. The Aral basin map.
Source: McKinney (2003).

deprived of the heat storage medium, this Central Asian region's (Figure 2) summer and winter became extreme. CO_2 effect was not reported to be responsible for the

Figure 3. Dying rivers feeding the Aral Sea.
Source: Micklin (2007).

Figure 4. The dried bed of the Aral Sea.
Source: User Staecker (2003).

generation of climatic extremity.

During1960 -2000, the basin's summertime average monthly air temperature increase vis-à-vis wintertime decrease was 2°C- 6°C per month (Zavialov, 2007). Also, summers were getting hotter and becoming short-lived whereas winters were getting colder and becoming long-lived along with decreased precipitations. Ragab-Prudhomme (2002) predicted temperature variations up to 2050. Micklin (2007) reported of the water body's drop in size, salinity increase drop in fish production, generation

Figure 5. Two and a half decade apart Aral Basin scenes - left side in 1989 and right side in 2014.
Source: NASA Collage by Producer Cunningham (2014).

of dust storms, and degradation of biotic communities. These were the USSR's self-infliction. Beyond the self-infliction by the surface water exploitation, coercive action has been taking place in the Ganges valley by pushing the lower basin to face the domino effects of upstream piracy by India. India killed the tributary-rich Hooghly River, a tributary of the Ganges, by building dams and barrages on the Hooghly's primary, secondar, and tertiary tributaries of the Hooghly. On the plea of restoring the navigability of the Calcutta Port located more than straight 252 km away from the Farakka point, India then built the Farakka Barrage upon the Ganges and started pirating the downstream Bangladesh ecosystem's elixir water under many tricks. The upstream water piracy took precedence over the dredging of the port. On top of this, India surrounded Bangladesh along the 4,096-kilometre-international border, the fifth-longest land border in the world, by a ring of dams and barrages upon more the half of the 59 common rivers between the two countries for water piracy in the lean season and inundation of Bangladesh during the flood season.

Indian chosen political party in Bangladesh does not protest against India's turning the affected river basins into deserts as well as inundation with unprecedented floods (https://www.thedailystar.net/environment/climate-crisis/natural-disaster/news/flood-sylhetsunamganj-50000-families-left-dark-3026651). In the country's National Assembly, the opposition party which is called the enemy party by the Bangladesh Premier is not allowed to raise the devastating flood issue for discussion.

That was India's treatment to her eastern neighbor. Her western neighbor Pakistan was threatened for cutting off water discharge voiding the World Bank-initiated Indus Treaty signed by the countries in the sixties of the last century. The Indus is the world's 19th longest river with a length of 3,610 km, has the world's 14th annual discharge of 2.7E8 cubic meters. The sources of river discharges in Pakistan lie in India.

Furthermore, China's dam building on the world's 9th largest and the 15th longest River Brahmaputra, and the Indian dam building in the Brahmaputra basin will dwindle the river. The Brahmaputra has the world's 4th largest annual discharge of 1.23E10 cubic meters.

In Southeast Asia and East Asia, the continued building of dams in the basin of the Mekong River (the world's 12th longest having the 7th annual discharge of 4.05E8 cubic meters) by China and the downstream countries will weaken the river.

The article demonstrates the politically motivated greed-driven anthropogenic actions-caused inland water bodies' depletion through water piracy from the feeding rivers to cause environmental heating vis-a-vis cooling. At the preliminary stage, the article lists some of the principal effects pertaining to the pre- and the ongoing piracy periods with illustrations highlighting the transitions. An integrated computer model development remains the goal.

MATERIALS AND METHODS

The author paid visits to the affected region to be an eyewitness of the environmental changes occurring in the lower Ganges basin. Photographs of dry surface water resources were taken. River discharge, climate, navigability, lightning, and other data were obtained from Bangladesh government offices, published literatures, and electronic and print news media. The environmental reactions rose gradually for continued deprivation of water in the lower courses of the Ganges River. The coerced water treaties between India and Bangladesh and their effects upon Bangladesh have been presented. Also, the Indian confining of water resources within herself and extreme climatic effects have been reviewed. The region's central climate office did not find any change in climate for not considering shorter time intervals of climate data in their analysis although people's feeling of the summer heat and the winter cold along with the climate center-recorded temperature figures were reported in the news media. About a decade of temperature data preceding and following the onset of the water piracy was selected for analysis because of the relevancy.

The annual summertime highest and the wintertime coldest temperatures vs years were plotted to find the onset of the heating and cooling. The annual hottest and the coldest temperatures were found for pre (prior to 1975)- and post-piracy to study the correlation with the Ganges discharges. The non-identically of the pre-piracy and the ongoing piracy period Ganges discharges was established by using K-S statistics (Hollander and Wolfe, 1999). The correlation of the pre- and ongoing piracy period HDD and CDD with the Ganges discharges for the same periods was studied. Also, analyses of rainfall, humidity, and lightning data were made. Responses of a prominent climatologist and a Nobel Laureate

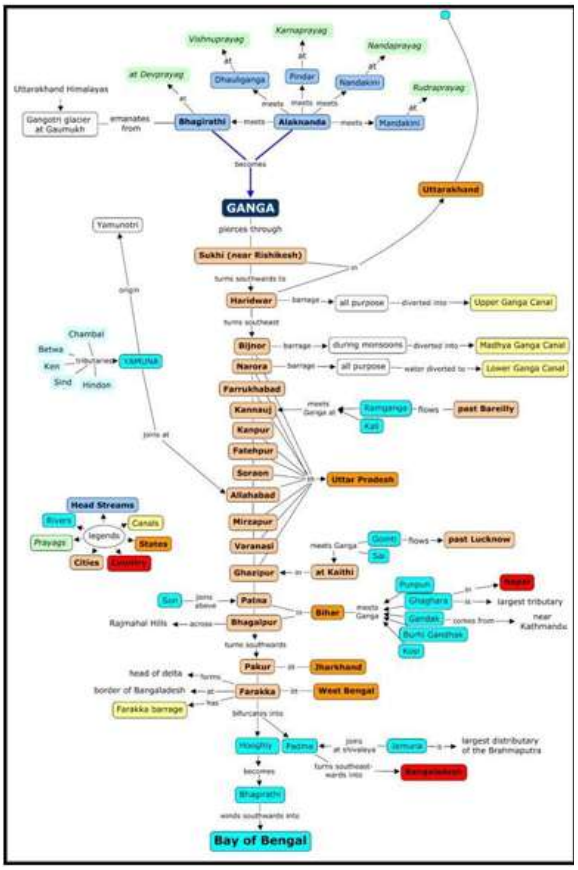

Figure 6. The Ganges's course from the source to the Bay of Bengal.
Source: National Mission for Clean Ganga (NMCG).

Figure 7. As India's Ganges runs out of water, a water crisis looms.
Source: Summer drying of the Ganga. Image by Abhijit Mukherjee, 2018).

Professor on the issue of upstream water piracy have been presented. The internationality of the sweet water resources has been touched

Figure 8. Shows the countries in the Ganges (India and Bangladesh), the Brahmaputra (China, India, and Bangladesh), the Indus (India and Pakistan), and the Mekong basins (China, Myanmar) (Map of India, 2012).

with the recommendation of no greed-based but need-based use of water by riparian countries to keep the planet livable.

RESULTS

The Ganges in India

Figure 6 shows the course of the Ganges from the birthplace to its forced fall (because India artificially changed its course) in the Bay of Bengal. Figure 7 shows the drying of the Ganges bed. At places, groundwater supplies the river water.

In Figure 8, the Nadia District Rivers (Figure 9) and the Damodar basin (Figure 10) fall in the yellow colored West Bengal to the west of Bangladesh. The Bhagirathi (Hooghly) river was fed by many mighty tributaries (Figure 10). Both Figures 9 and 10 show the Hooghly basin. India started damming the primary, secondary, and tertiary tributaries of the Hooghly River from the fifties. The river was almost dead. India then built the Farakka Barrage (Figures 11 and 12) on the Ganges in 1975 on the plea of turning the Calcutta Port, located more than 250 km away downstream, navigable, although dredging the port was the right solution. She dug the Feeder Canal (Figure 13) to let the Ganges discharge down it. Then she publicized that the Ganges changed its course through Hooghly to

Figure 9. Nadia District Rivers.
Source: Niyogi (2002).

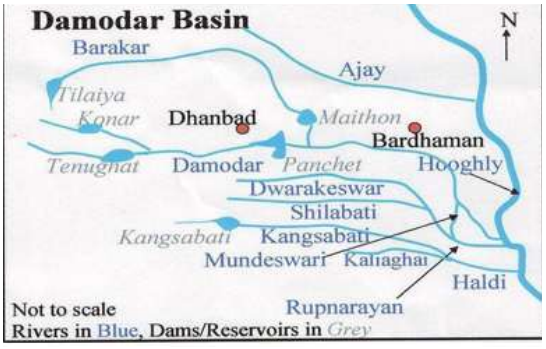

Figure 10. Damodar basin.
Source: Niyogi (2008).

Figure 11. Ganges River showing the Feeder Canal to the left. Source: (Google My Maps, 2023)

Figure 12. The 2,245 m long Farakka Barrage with 109 gates, 18.30 span, and 76,500 cumecs discharge capacity upon the Ganges (courtesy of SANDRP – South Asia Network on Dams, Rivers and People) Thakkar (2017).

fall in the Bay of Bengal. There have been coerced water sharing treaties (Table 1 and Figures14 and 15) between India and Bangladesh from time to time, and in between, India pirated inordinate amounts of Bangladesh ecosystem's water (Adel, 2015) (Figures 16 and 17). Most of the Ganges River's dry season flow is taken by

Figure 13. The 38.38 km long Feeder Canal that originates in the upstream of the barrage with a discharge capacity of 1,132 cumecs (Photo credit: Prasad, reproduced with permission).
Source: Author.

India (Hillary, 1979). The Gangetic ecosystem cannot survive the India's rationing of water to it.

The coercive treaties

Figures 14 and 15 compare the water sharing under the coercive 30-year treaty signed by the current Bangladesh government which holds power at the mercy of India. The current government is totally speechless under India's desertification of Bangladesh as well as under inundation of Bangladesh, and she does not like to hear complaints against India. Tables 2 and 3 show the water sharing under the current coercive treaty which will expire in 2027. Bangladesh has got ever decreasing dry season discharge, and India has got the ever-increasing dry season discharge. The drooping dry season flow has had dire effects, one of the most damaging of which is the inland intrusion of salty water fronts, which cannot be pushed back into the ocean and have caused the salinization of coastal areas, leading to the death of freshwater aquatic life (Figure 23).

The Padma's (Ganges's) condition in Bangladesh

In course of time, apart from pirating the Ganges water, India surrounded Bangladesh by a unique ring of dams and barrages which is known as the Great Ring of Dams and Barrages (Figure 16) covering more than 30 of the 58 common rivers. Consequently, the lower Ganges basin (Figure 17) has transformed into the Aral Sea basin-like environment. More than 70% of the Ganges's discharge is being pirated as shown in the annual discharge (Figure 18).

The broken own monthly discharge for some remarkable years is very much appalling (Figure 19).

Figure 20 shows the historical discharge of the Ganges at the Hardinge Bridge point, 233.5 km away from Farakka through Rajshahi – Nawabganj. A water resources engineer said that the government had setup a discharge monitoring station near the Hardinge Bridge point where ground water supplies the river water so that any Indian violation of the current treaty remains masked. A huge shoal has formed on the Ganges (Padma) bed further downstream in the lower Ganges basin (Figures 21 and 22) from the ring of dams and barrages in Bangladesh (Katz, 2008). Figure 23 shows the cracked bed of the Ganges under the Hardinge Bridge.

Hafiz (2023) reports of more than 500 large and small dams on the 47 transboundary rivers that has dried 158 rivers, canals, and floodplains.

The Ganges's (Padma's) distributaries' conditions

Figures 24 and 25 show rivers of North Bengal and the basins of the Baral, the Ganges's primary distributary (Figures 26 to 28), and the Musa Khan, the Ganges's secondary distributary. The Baral is approximately 147 km long, 120 m wide, 6 m deep. The upper basin of the Baral had a drainage area of 230 square km. Figures 26 through 28 shows the current conditions of the Baral.

The Baral's distributary Musa Khan's (Figures 29 through 31) discharge of about 1,000 m^3/s during the flood season has been totally stopped by the formation of a shoal that level off the riverbed with its banks. About 15-km Musa Khan would feed its floodplains during July through November using 50 canals. Those floodplains do not get a single drop of water from the Musa Khan. These dead tributaries were playgrounds of Gangetic dolphins (Figures 32 and 33) for at least four months of the year. India wiped out the habitats of these aquatics.

The Gahrai distributary

The Garhai-Madhumati River is the lifeblood of southwest Bangladesh. It has sixteen distributaries. In 1988 summer, its mouth was clogged, and no water could flow in it. In the upper reaches, the river is known as the Madhumati and in the lower reaches, the Garhai. Figure 34 shows the summertime scene of the river with shoals on its bed. The gradual decreasing Ganges's discharge-dependent flow in the Gahrai is shown in Figure 35.

Figure 36 shows the Gahrai catchment in southwest Bangladesh. Figure 37 shows the historical discharge of the Gahrai.

The Teesta basin

Figure 24 shows that 315-km long Teesta rises in the

Table 1. Upstream's India's Increased Allocation (cumecs) in the Coercive Water Sharing Agreements.

Period	Provisional (4/21-5/31/75)	5-year (1977-82)	30-year (1997-2027)
April 21-30	311.5	566	735.6
May 01-10	339.6	608.5	990.5
May 11-20	424.5	679.2	1.092
May 21-30	452.8	757	1.132

Source: Sattar (1998).

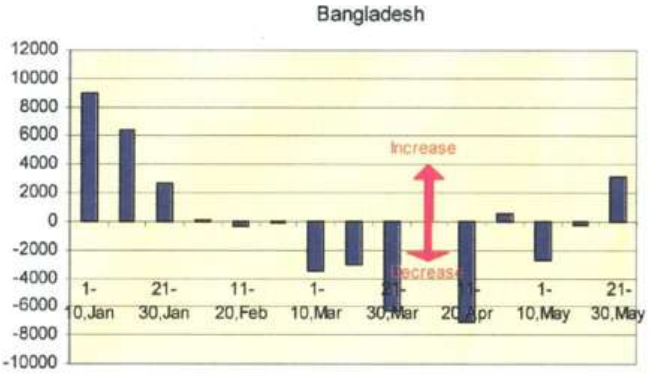

Figure 14. In 1996 coerced piracy authorization by Bangladesh that shows ever-decreasing dry season water share for her relative to the 1977 water piracy agreement
Source: Author.

Figure 15. According to 1996 coerced piracy authorization, India has got the ever-increasing dry season discharge relative to the 1977 water piracy agreement.
Source: Author

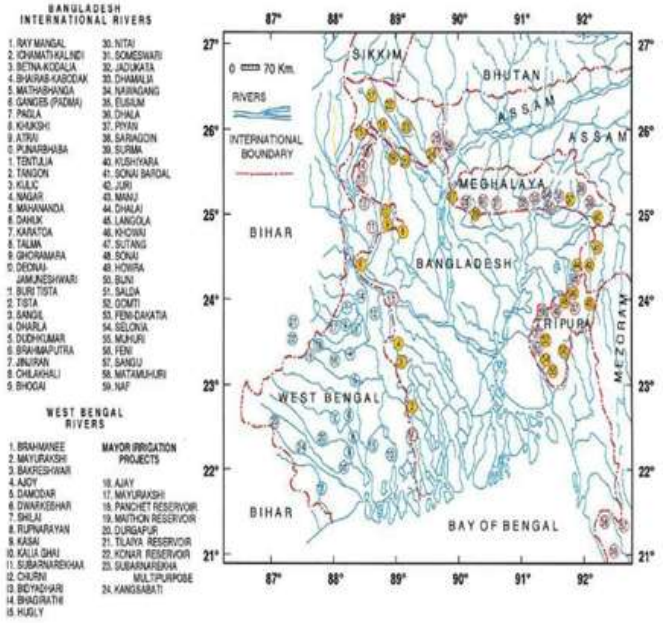

Figure 16. Bangladesh encircled by Indian Great Ring of Dams and Barrages marked in yellow colors, a unique technique to subjugate a downstream riparian nation.
Source: Adel (2002).

eastern Himalayas, flows through West Bengal and Sikkim states of India to meet the Brahmaputra in Bangladesh. It drains 12,370 square km. Whereas the Teesta River needs 4,000 cusecs for its existence, its lowest discharges have been 4494, 4732, 529, 8, and 42.45 to 11.57 m3/s in 1980, 1990, 2000, 2005, and 2014, respectively (http://archive.thedailystar.net/2006/11/03/d611031803114.htm).The Teesta's bed has formed 58 shoals (Figures 38 and 42). It brings down a lot of silt from the upstream (Figure 39). Its silted bed causes people's sufferings by flooding (Figures 40 and 41; https://www.facebook.com/100077351871549/videos/731548061424597). The Indian Teesta Dam is shown in Figure 43.

In the pre-piracy period, flood and rainwater-filled numerous shallow and deep floodplains and other surface water resources would work to recharge the groundwater annually. In the ongoing piracy period, people use groundwater in all sorts of water-related works – drinking,

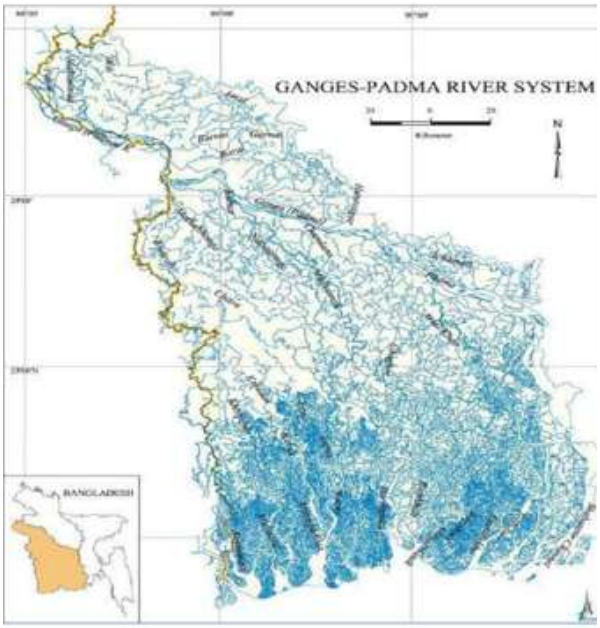

Figure 17. The Ganges basin in Bangladesh.
Source: Banglapedia, 2021a.

cooking, cleaning, bathing, gardening, aquaculture, agriculture, irrigation, etc., while there is little recharging of groundwater annually from rainwater and that more than 40% of the withdrawn water evaporates. Irrigation sector is the major user of groundwater. The countrywide irrigation sector uses deep tubewells, shallow tubewells (Figure 44), low lift pumps, manual pumps, and indigenous water lifting devices (https://www.google.com/search?sxsrf=ALeKk03q6d8Y4SloIxOmQaJ2N-fF3eEf3A:1626373742979&source=univ&tbm=isch&q=irrigation+in+Bangladesh&sa=X&ved=. Consequently, the groundwater table the buildup of which takes thousands of years (Figure 49) (Dey et al., 2013) is depleting. Shallow water tables do not exist anymore. People had to reset their tubewells to withdraw groundwater from a depth of 80 meters or more. This depth is more than 8 times the pre-piracy period setup depth. During the on-going piracy era, a huge number of tube wells have been abandoned for withdrawing no water or arsenic contaminated water (Figures 45 to 48). Arsenic contaminated groundwater (Adel, 2013) drinking accounts for a 20% fatality.

Floodplains

Canals from rivers would feed the floodplains which would work as the recharging wells for the groundwater. Insufficient rainfalls fail to recharge the groundwater. Groundwater extraction overcomes recharging. Water cannot accumulate in canals and floodplains where people used to swim in the pre-piracy period. Table 4 highlights the differences between the pre-piracy and piracy era important environmental issues.

Climatic extremity

Figures 50 and 51 show the negative correlation between discharge short fall and the summertime temperature rise, the correlation coefficient being -0.60. Figures 51 and 52 show the positive correlation between the shortfall of the Ganges discharge and the wintertime temperature fall. They are positively correlated with a correlation coefficient of 0.55. Figures 53 shows the rising HDDs and CDDs. Their positive correlation coefficient with the Ganges discharge shortfalls are 0.47 and 0.49, respectively.

Humidity

The humidity variations (Figures 54 and 55) are due to the massive groundwater withdrawals more than 40% of which evaporates. The average maximum humidity during the pre-piracy period was 90.21% and in the ongoing piracy period 92.54%. The average minimum humidity was 55.2% in the pre-piracy period, and in the ongoing piracy period it is 52.9%. The highest relative humidity appeared 1635 times during the pre-piracy period, and it rose to 2957 during the ongoing piracy period. The median and mode values for both the maximum and minimum remain unchanged except for the 5% increase of the minimum humidity mode during the ongoing piracy period.

Precipitations

Precipitation (Figures 56 and 57) has decreased. In pre-piracy days, there would be varying degrees of weeklong rainfalls in the months of June, July, August, and September. This would help for recharging groundwater. In the ongoing piracy period, light rainfall frequency has increased but the heavy rainfall frequency has decreased.

Crops burning

Paddy cultivation has been affected by the shortage of rainfall along with the scorching heat. Figure 58 shows the condition of a paddy field in the Ganges basin.

Increased lightnings

Figures 59 and 60 show exceedingly increases of cloud to

Table 2. Coercive piracy formula.

Water availability at farakka (cumes)	India's share (cumes)	Bangladesh's share (cumes)
1.981 or less	50%	50%
1.981- 2.125.5	remainder	990.5
2.122.5	1.132	remainder

Source: Sattar (1998).

Table 3. Water sharing in the coercive treaty.

Internal (days)	Average discharge (1949-88) (cumes)	Pirated quatity (1949-88) (cumes)	Bangladesh' share (cumes)
Jan 01-10	3.042.70	1.132	1.910.70
Jan 11-20	2.764.15	1.132	1.632.15
Jan 211-30	2.551.36	1.132	1.419.36
Feb 01-10	2.442.94	1.132	1.310.94
Feb 11-20	2.344.91	1.132	1.212.91
Feb 21-28	2.238.70	1.132	1.106.70
Mar 01-10	2.106.06	1.115.56	990.50
Mar 11-20	1.950.75	960.25	990.50
Mar 21-31	1.830.67	990.50	840.17
Apr 01-10	1.787.99	797.49	990.50
Apr 11-20	1.772.51	990.50	787.01
Apr 21-30	1.726.07	735.57	990.50
May 01-10	1.906.03	990.50	915.53
May 11-20	2.082.60	1.092.1	990.50
May 21-31	2.316.47	1.132	1.184.47

Source: Sattar (1998).

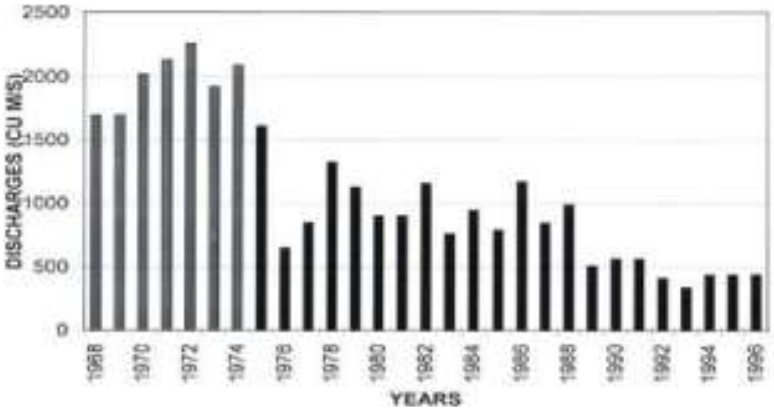

Figure 18. The drastic drop in the Ganges discharge in Bangladesh.
Source: Hebblethwaite (1997).

ground lightnings. 2018 has been the worst year (Figure 59) and May has been the worst month of any year (Figure 60). There has not been any kind of indoor or outdoor engagements in which lightnings do not strike any victims (Adel, 2021). Some lightnings victims are pictured in Figures 61 and 62.

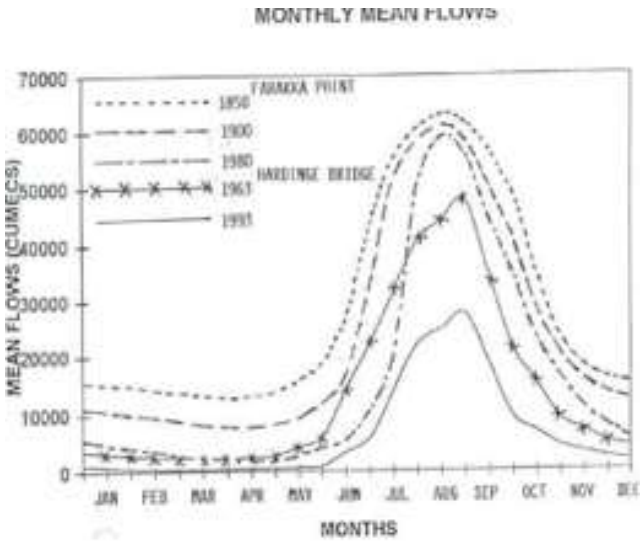

Figure 19. Monthly average discharge in the Ganges. The ecosystem that once survived with the discharges indicated by the top three curves has to survive now with the discharge indicated by the bottom curve or less than this.
Source: Adel (2002).

Potential aral Sea Basin-like scenes

China completed 510 MW Zangmu Dam on the upper reaches of the Brahmaputra, a few kilometers from Bhutan—India border. Its active capacity is 86,600,000 cubic meters. Three more dams are under construction – Dagu (640 MW), Jaicha (320 MW), and Jeixu. The largest dam on the Brahmaputra the Zam hydropower station was completed in 2015. (https://timesofindia.indiatimes.com/india/china-plans-dam-on-brahmaputra-how-it-may-impact- india-bangladesh/articleshow/79528597.cms). China is now setting up hydropower plants in the Brahmaputra's lower reaches (Figure 63).

India is competing with China – she will build the India's largest and world's tallest 288-meter high concrete gravity dam with a 10 gigawatt capacity, the Dibang Dam in Arunachal Pradesh.

India's Central Electricity Authority (CTA) foresees her northeastern region as the country's future powerhouse (Figures 64 and 65). The agency selected 168 large hydroelectric project sites in the Bhahmaputra basin in 2001. The expected power output would be 63,328 MW (https://thediplomat.com/2020/12/india-to-expedite-dam-construction-after-china-announces-project-in-tibet/). The Brahmaputra-Jamuna Subbasin is shown in Figure 66. Further, The Brahmaputra is 13 km wide (Figure 67). Its lowest flow ever recorded is 3,117 cumecs. The piracy of an unknown quantity of water from the Brahmaputra will have a more disastrous effect than in the Ganges basins basin (Sufian, 1993; Sattar, 1996).

Western neighbor of India: The Indus basin

Apart from the Indian threats her eastern neighbor Bangladesh faces, the western neighbor Pakistan faces even a serious threat of receiving no water from India cancelling the WB-mediated Indus Treaty signed by the governments of Indian and Pakistan in the sixties (Figure 68). According to the treaty, Pakistan gets water from the Indus, the Jhelum, and the Chenab Rivers. And India gets water from the Ravi, the Beas, and the Sutlej Rivers (Figure 69). About 39% of the Indus River system lies in India and 47% in Pakistan (FAO, 2011). Pakistan's one of the most water-stressed countries. Pakistan's water demand is projected to be 225 cubic kilometers in 2050 which was 163 cubic km in 2015. Pakistan fears India's upstream Indus water piracy through dams, which it has already attempted to prevent multiple times due to its contravention of the Indus Waters Treaty. India gets the upper hand in upstream water piracy by building dams and barrages (Figures 70 and 71) for which there are no restrictions in the IWT, nor is there a restriction on the quantity of water stolen (https://climate-diplomacy.org/case-studies/water-conflict-and-cooperation-between-india-and-pakistan; Dutta, 2019; Thakkar, 2017).

India faces extreme climate events, possibly, because of confining water by many dams and barrages in Uttarakhanda (Adel, 2018). India's progression of irrigation and lightning strikes correlates as evidenced from Figures 72 and 73.

Mekong basin

Figure 74 shows the Mekong basin hydroelectric project sites including the operational, under-construction, and planned ones (Table 5). The downstream countries face worsening drought situation due to China's inclination for dam constructions (https://www.stimson.org/2020/new-evidence-how-china-turned-off-the-mekong-tap/). This is the same scenario of precipitation as in the Ganges basin discussed above. But China disputes the issue.

DISCUSSION

Downstream sedimentation

When the river barrage's outlets are opened following failure to accommodate water, stream discharge and velocity increases, the smallest, lightest, and most nonrounded particles are the first to be dislodged from the bed and carried in suspension in the stream. This period is very short lived. When the stream velocity begins to drop, the largest, the heaviest, and the roundest particles are the first to return to the riverbed. This is the longest lived period.

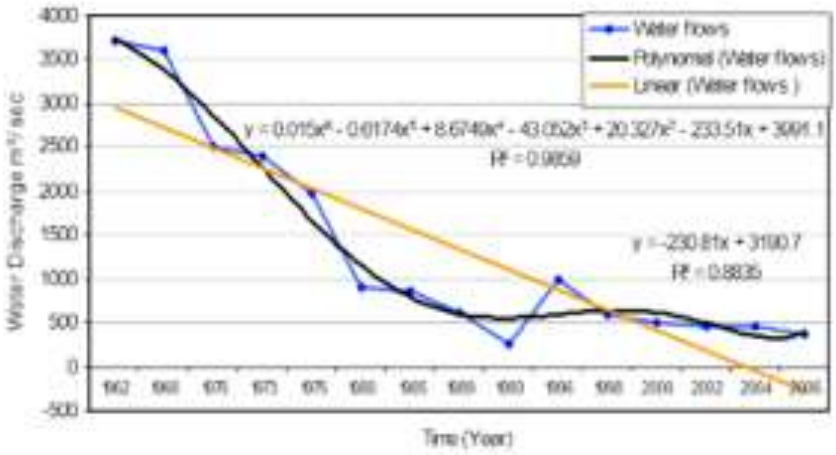

Figure 20. The Historical Ganges Water flows in the Harding Bridge point.
Source: Islam and Gnauck (2011).

Figure 21. River Ganga (Padma) dried up & reduced to a 6ft wide shallow stream in Rajshahi, Bangladesh.
Source: Katz (2008).

Figure 23. The 1.8 km long Hardinge Bridge on the dry River Padma (Ganges) at Paksey, named after India's British Viceroy Lord Hardinge (1910-1916)
Source: Shakoor, personal communication, (1999).

Figure 22. Cracked bed of the Ganges in Rajshahi].
Source: Katz (2008).

Figure 24. Main Rivers of North Bengal.
Source: Niyogi (1997).

Figure 25. The Baral and the Musa Khan basins.
Source: Adel (2002).

Figure 26. A huge shoal in front of the Baral's origin.
Source: Author

Figure 27. The pasture on the Baral.
Source: Author.

Figure 28. A bridge upon the dry Baral River
Source: The Daily Amar Desh.

Figure 29. The Baral's offshoot Musa Khan with the clogged origin; the Musa Khan's origin is levelled off with the bank.
Source: Author.

Figure 30. The Musa Khan under a bridge.
Source: Photo credit: Samad, personal communication (1999).

There are several reasons for the downstream sedimentation following upstream dams and barrages. If

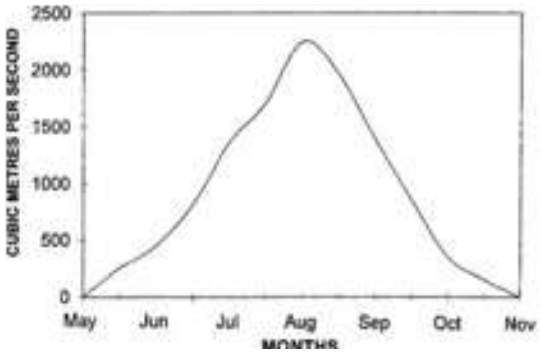

Figure 31. The Musa Khan's estimated hydrograph which was about one-third of the Baral's hydrograph.
Source: Adel (2002).

Figure 32. Image of a Ganges dolphin. These dolphins would populate the distributaries of the Ganges.
Source: Sinha (2021).

Figure 33. The carcass of an Irrawaddy dolphin lies on the Kuakata beach in Bangladesh's Patuakhali district, May 14, 2022.
Source: Courtesy of Chowdhury from Dolphin Conservation Committee of Kuakata, Bangladesh, (2022).

the downstream becomes wider than the upstream, discharge speed weakens allowing the time for sedimentation according to the equation of continuity:

$$v_{dn}=(A_{up}/A_{dn})v_{up} \quad (1)$$

Figure 34. The summertime condition of the Gahrai, the main distributary of the Ganges that used to feed its 16 distributaries.
Source: The Daily Star, October 21, 2014**,**

where: v_{dn} = Velocity at the downstream; v_{up} = Velocity at the upstream; A_{up} = River area of cross section at the upstream; A_{dn} = River area of cross section at the downstream

Also, downstream distributaries weaken the parent river current because of the current division. Figure 75 shows widening of the Ganges as it moves past West Bengal border.

Experiments on fluid sediment mixtures have shown that an increased suspension concentration causes a substantial reduction of settling velocity (Woo et al., 1988; Mazumder, 1994). Upstream beside the barrage, particles get some settling time as has been observed for the Farakka Barrage.

Near the origin of distributaries, the parent river's flow is weakened due to the stream division, which affects the cosine of the angle the distributary bifurcates at. This further favors siltation. The decrease in speed at the point of changing stream direction in the distributary allowed the sediment to accumulate and form sedimentary hills at the origins of the Baral, Musa Khan and Gahrai Rivers, thus clogging them.

Floodplains drying and sinking groundwater table

For the pre-piracy era

The total water balance of the basin is determined by the precipitation (about 1.5 m/year), the inflow to the basin (about 0.5 m/year) via rivers and canals, the subsurface inflow from groundwater movement (GW), and the water withdrawal from underground and surface water bodies (about 5 mm/year with a factor of 0.6 representing 60% infiltration for the withdrawn water, W).

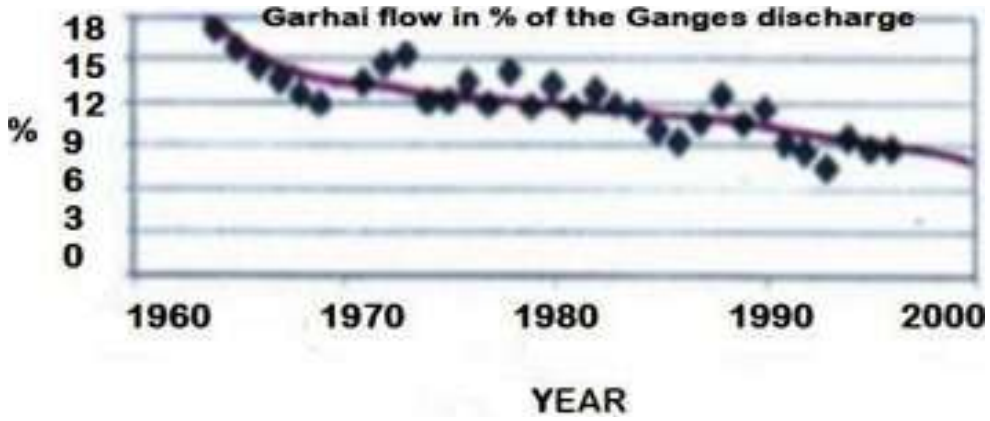

Figure 35. Decreasing trend in the Garai's discharge.
Source: Hossain et al., personal communication (2003.

Figure 36. Gorai River catchment area in south western region in Bangladesh
Source: Islam (2011).

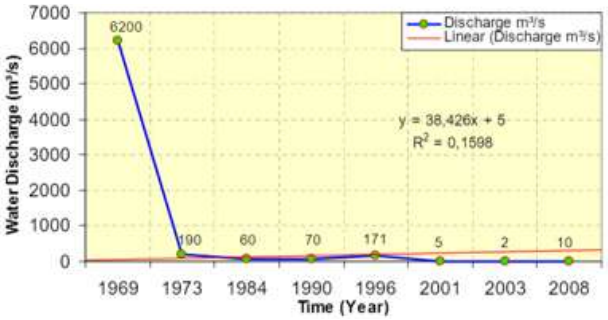

Figure 37. Water discharge of Gorai River (1969-2008).
Source: Islam (2011).

Figure 38. 58 shoals on the Teesta bed.
Source: Roy, 2014).

Ongoing piracy era

The inputs to the system include stored surface and ground water (STRG), subsurface outflow from groundwater movement (GWout), and evapotranspiration (about 2 mm/year) (E). For all dried-out distributaries' basins, the stored surface and ground water together is equal to the precipitation (about 1.5 m year-1) minus evapotranspiration (about 2 mm year-1) and 0.4W.

$$STRG = P - E - 0.4W \quad (2)$$

Currently, the evapotranspiration E is more than 2 m $year^{-1}$, precipitation is less than 1050 mm yr^{-1}, and dependence on groundwater is more than ten times which explains the downward trend of the groundwater.

Figure 39. Silts clogged the Teesta Barrage gates
Source: The Daily Janakantha, Staff reporter, July 18, 2020). https://www.dhakatribune.com/bangladesh/319168/teesta-flowing-above-danger-level-all-barrage

Figure 40. Present a thumbnail view of the devastating flood situation.
Source: https://m.somewhereinblog.net/mobile/blog/dhabian/30337144

Figure 41. Present a thumbnail view of the devastating flood situation.
Source: https://m.somewhereinblog.net/mobile/blog/mostofa_kamal/30206906

Figure 42. The Teesta's dry silted
Source: https://www.thedailystar.net/teesta-to-affect-indo-bangla-relations-21336

Figure 43. The Teesta Barrage (Beautiful Bangladesh, 2012)

Figure 44. Irrigation by shallow tubewells from a depth of about 30 m (Courtesy of Banglapedia, 2021b)

Heating and cooling

Currently, the Ganges discharge water is about 40% of pre-piracy period discharge. Ganges's distributaries are dry. Floodplains and other surface water bodies are 50% of the pre-piracy period. Water medium has the highest specific heat. Clear water absorbs 90% of the incident radiation and reflects just 10%. Wet soil, at most reflects 20% of the incident radiation. The release of CO_2 of specific heat at constant pressure 846 J/Kg.^{O}C (https://www.engineeringtoolbox.com/carbon-dioxide-d_974.html) is beside the point in this scenario. In the pre-piracy days, it would absorb heat during the summertime

Figure 45. Deserted hand tubewells either fail to extract groundwater or yield arsenic-contaminated water.
Source: Photo credit: Samad 2003, personal communmication)

Figure 46. Deserted hand tubewells either fail to extract groundwater or yield arsenic-contaminated water.
Source: Photo credit: Samad, 2003, personal communmication

Figure 47. Deserted hand tubewells either fail to extract groundwater or yield arsenic-contaminated water.
Source: Photo credit: Samad, 2003, personal communmication

Figure 48. Deserted hand tubewells either fail to extract groundwater or yield arsenic-contaminated water.
Source: Photo credit: Samad, 2003, personal communmication)

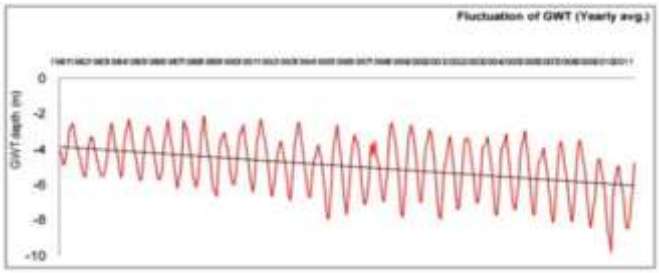

Figure 49. Shows how the groundwater in the north of Bangladesh is declining.
Source: Dey et al. (2013).

and retain it for release during the wintertime. In the absence of water bodies, there is no heat-absorbing and heat-retaining medium. Dry landmasses reflect heat amplifying its intensity. The absence of the heat-releasing water bodies in the wintertime, the temperature drops. Adel et al. (2014) estimates about 18 million trillion calories of heat cannot be trapped annually due to the upstream water piracy.

The huge pool of water that would be contained in place of the shoal of width 1.6 to 8 km in the Ganges and in other dried rivers could store a significant amount of heat letting not the rise of summer heat and dropping of winter cold. Summertime this huge sandy shoal has an emissivity of 90% (https://www.thermoworks.com/emissivity-table) and the average reflectivity of sand can be taken as 40% in the wavelength range of 500-800 µm (Drakopoulos et al., 2014).

The negative correlation coefficient shows moderate correlation between water shortage and the warming. So does the positive correlation coefficient between the

Table 4. Pre-piracy and ongoing piracy period highlights.

Issues	Pre-piracy period	On-going piracy period
Ganges discharge	1932±228 m^3/s	769±284.5 m^3/s
Floodplain water level	-	50% of pre-piracy level
Pon water level	-	50% of pre-piracy level
Groundwater table	-	Sinking by at least 0.5 m/s
Highest maximum temperature (°C)	37	45.1
Median maximum temperature (°C)	25.5	28.5
Mode maximum temperature (°C)	31	32
Average maximum temperature (°C)	29.8	30.8
Annual Htng Deg days (°C)	HDD	1.3 times more than HDD
Highest minimum temperature (°C)	8°C	< 5
Median minimum temperature (°C)	17.5	17.0
Mode minimum temperature (°C)	26.0	25.0
Abverage minimum temperature (°C)	20.3	19.8
Annual Clng. Deg days	CDD	1.44 times more than CDD
Highest RH Frequency	1635	2957
Average maximum RH (%)	90.21	92.54
Median RH (%)	72.5	72.5
Mode RH (%)	95	95
Average maximum RH (%)	55.2	52.9
Median RH (%)	52.5	52.5
Mode RH (%)	65	70
Light rainfall	Less occurrences	More occurrences
Heavy rainfall	>100 mm	50% Less occurrences
Monthly average rainfall	-	30% droppage
Ganges discharge correlation with His, Los, HDDs and CDDs	No correlation	Correlation coefficients are -0.60, 0.55, 0.47 and 0.49, respectively
Floodplains having water (km^2)	44,043	11,011
Heat content (calories)	1.71E19	4.32E18
Smr Ht excess and winter loss	-	10 times the pre-piracy
Lightning occurrences	-	Exceedingly increased, spotlighted by int'l news media
Ganges's 794 million tons sediment	-	49% deposition on Indian coast, 5% on Bangladesh coast
Inland Deposition	-	8% on Indian floodplains, 41% on Bangladesh riverbeds
Navigability loss	-	1200 km waterways dry summertime
Saline Water Intrusion		1 ppt has increased to 20 ppt over wider areas

Source: Updated from Adel et al. (2014)

water shortage and the cooling down.

Relative humidity

In the absence of water bodies, relative humidity has been affected by the withdrawal of the huge quantity of groundwater in the presence of little or no recharging water. Almost two time's rise of the maximum humidity which occurs in summertime is likely to be related to the shallow level groundwater withdrawal for rice cultivation. The rise of the maximum relative humidity level is also related to the widespread groundwater withdrawal. People suffer from the rising temperature and rising relative humidity.

As to the humidity variations, it is the evaporation from the extracted groundwater that adds to the piracy period humidity. Irrigated lands have shallow water levels. The solar radiation heats up a smaller volume of water raising its temperature at the surface faster. At the surface, the specific humidity becomes low and favors further evaporation.

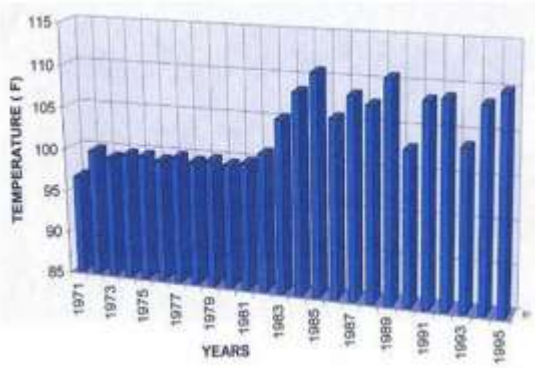

Figure 50. Annual maximum temperatures.
Source: Adel (2002)

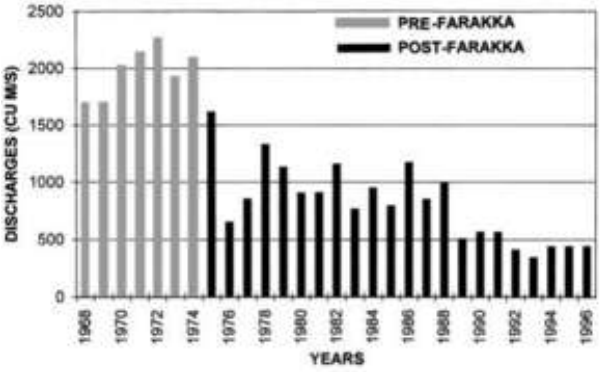

Figure 51. The Ganges's discharge in Bangladesh.
Source: Hebblethwaite (1997).

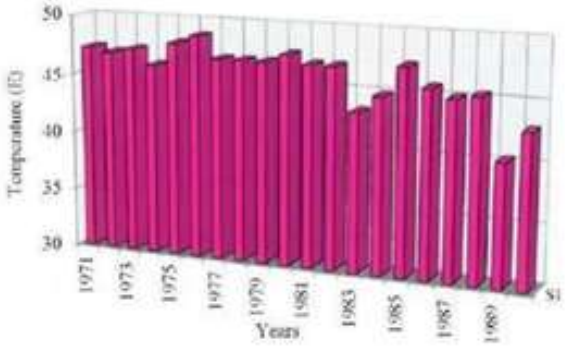

Figure 52. Shows the annual minimum temperatures.
Source: Adel (2002).

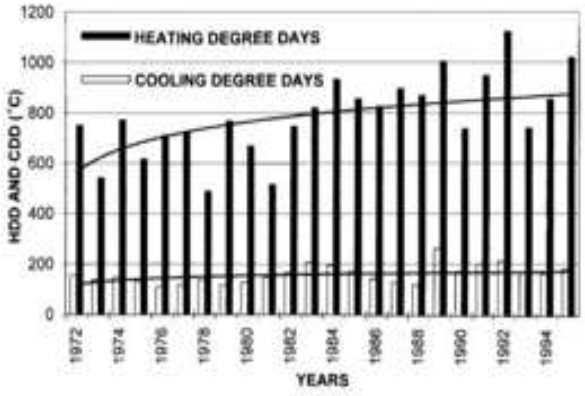

Figure 53. Shows the plots of HDDs and CDDs.
Source: Adel (2002).

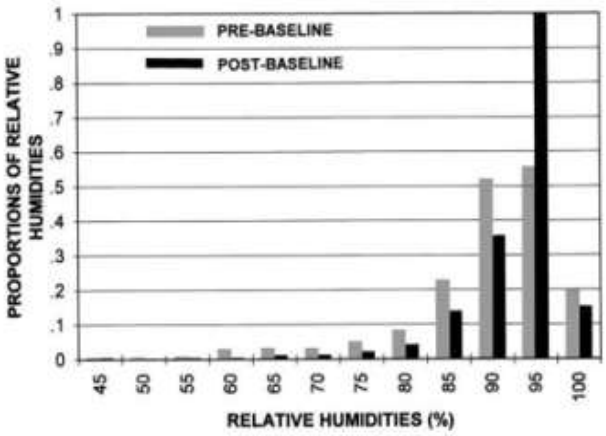

Figure 54. Variations of the maximum relative humidity during the pre-piracy and the ongoing piracy periods Source: Adel (2002).

Rainfall

Regarding the drop in precipitation, it can be said that water begets water. There are more rainfalls on oceans than on lands. The moisture-laden air coming over the land from sea does not meet the adequate moisture to fulfill any critical condition to cause rainfall.

Crop burning

Rice plants reflect more than 40% and absorb about 60% of the incident radiation. Green crops reflect 30% of the incident radiation. The specific heat capacity of rice field's environmental materials like air, wet soil, dry soil, and sand are 1,005, 1,480, 800 and 830 J/kg.°C, respectively. The materials favor longer duration high temperatures around the rice fields under the scorching heat of the Sun. The burning of rice plants in the field could be related to hot weather that affects the photosynthesis by accelerating some chemical reactions and retarding others

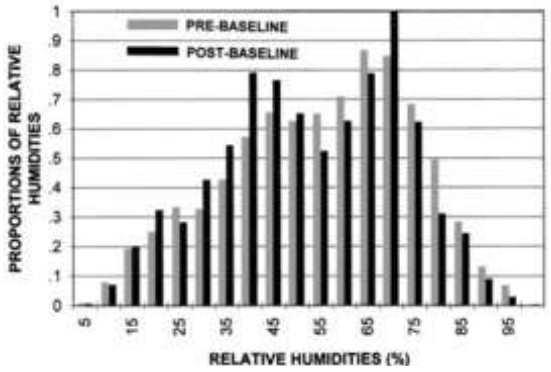

Figure 55. Variations of the minimum relative humidity during the pre-piracy and the ongoing piracy periods. Source: Adel (2002).

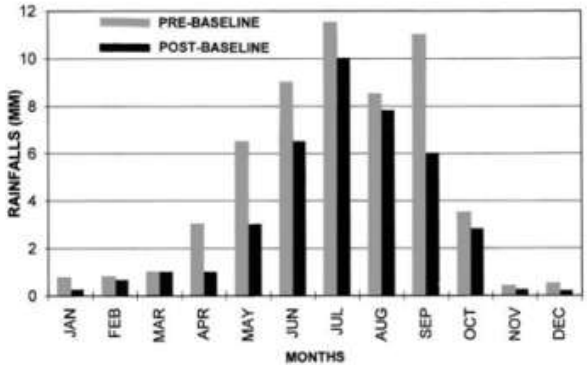

Figure 56. Comparison of monthly rainfalls.
Source: Adel (2002).

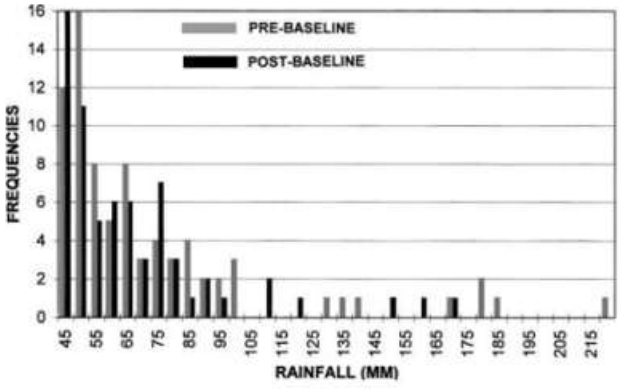

Figure 57. Decreased rainfall frequencies.
Source: Adel (2002).

(https://www.science.org/content/article/rice-genetically-engineered-resist-heat-waves-can-also-produce-20-more-grain).

Figure 58. Rice field burning.
Source: Zaman (2021).

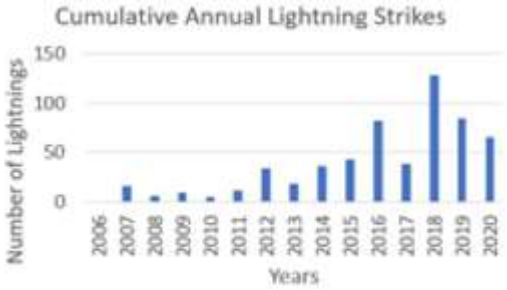

Figure 59. Annual number of lightnings.
Source: Adel (2021)

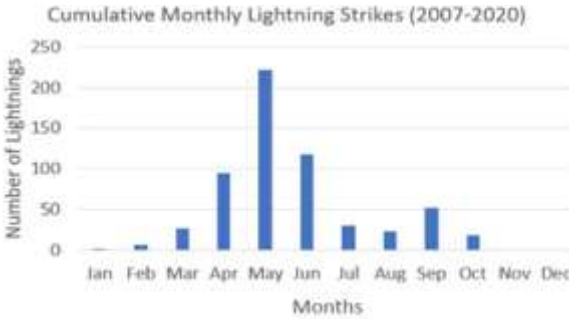

Figure 60. Maximum lightnings occur in May.
Source: Adel (2021

Figure 61. Four farmers died of lightning strikes while working in a rice field in Magura source: Magura Representative (2018).

Figure 62. Ten buffalos died of lightning strikes in Sirajganj (Sirajganj Representative, 2018)
Source:https://bangla.bdnews24.com/samagrabangladesh/article1491890.bdnews).

Figure 63. The great curving of the Brahmaputra, the site for China's world's biggest hydropower project.
Source: BBC NEWS (2014).

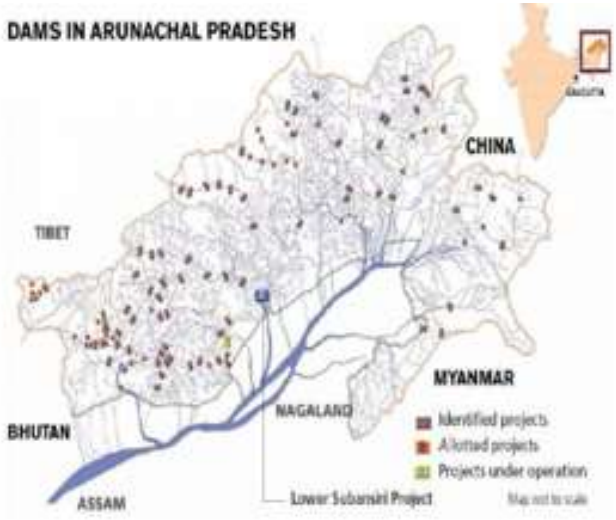

Figure 64. Identified, allotted and operational projects in Arunachal Pradesh
Source: (Bosshard, 2011).

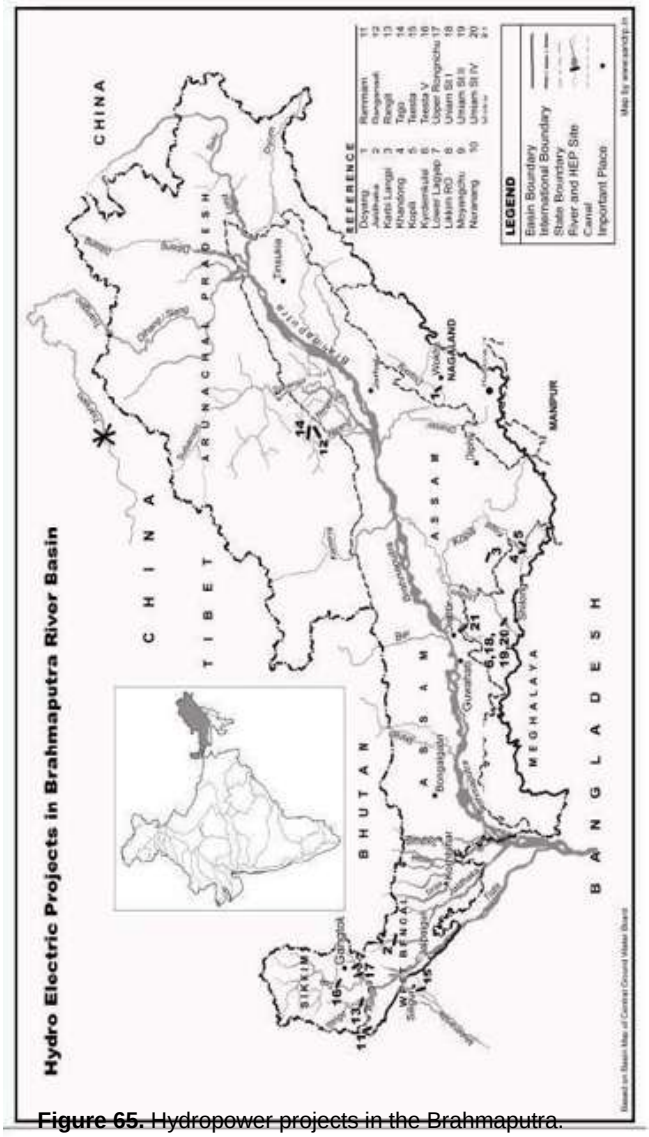

Figure 65. Hydropower projects in the Brahmaputra.
Source: Adel (2018).

Lightning

Each degree rise in Celsius temperature causes a 12% increase in lightnings (Romps et al., 2014; Thompson, 2014). At least, a rise of 4°C temperature has been observed in the Ganges basin in summer. For a linear relation, the increase in lightnings may be about 50%. There has been a rise of relative humidity following the temperature increase. Bangladesh's Meteorological Office reports that prior to 1981 the country had on average nine days each May lightning's strikes. Afterwards, the figure has risen to 12 days each May (https://in.reuters.com/article/bangladesh-lightningisaster-idINKCN0Z81U4). Reasons are related to the victims' wet body conductivity increase by 100 times, crops' leaves/thorns conductivity in the range of ~ 0.3 to

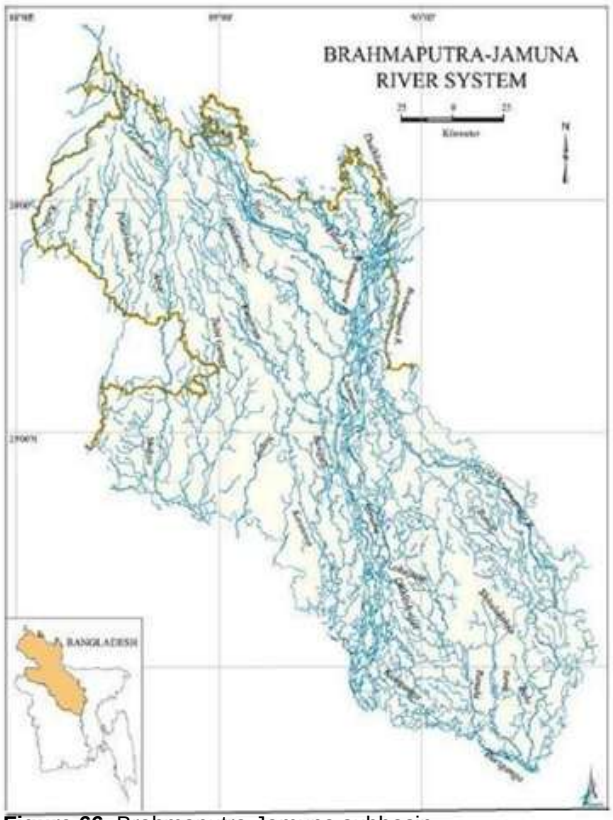

Figure 66. Brahmaputra-Jamuna subbasin.
Source: (Courtesy of Banglapedia, 2021c).

Figure 67. The Brahmaputra in Bangladesh.
Source: Hoque (2014)

0.9 S/m, curvature-dependent induced electric field in victim' working tools and/or ornaments of conductivity ~ 10^{-1} to 10^{-1} S/m in an aerial environment of increased electrical conductivity in the range 10^{-14} to 10^{-9} S/m due to a past, ongoing, or sudden shower when the aerial electric field becomes about 20 times larger than the natural one of 100 V/m (Adel, 2021).

Figure 68. Indian Prime Minister Narendra Modi's threat to Pakistan of cutting off the water supply.
Source: https://www.indiatoday.in/india/story/pm-modi-s-water-threat-to-pakistan-what-india-can-do-under-indus-waters-treaty-1609883-2019-10-16, Photo: PTI.

China and the downstream countries in the Mekong basin have been exploiting this river discharge. People will feel little by little the climate change – increased heating vis-à-vis cooling (Adel et al., 2014).

Nobel Laureate's wrong view

The author asked Niepold (2018) from NOAA Climate Program Office about the reality of the climate change due to surface water resources exploitation at the American Meteorological Society's Climate Studies Diversity Project Workshop in Silver Springs, MD (https://drive.google.com/drive/u/1/folders/1xTdAnDqlyn_dcMdDqID2TdC12UQv3-Sf)). He admitted the reality but was unable to address the issue due to many factors. The Nobel Laureate from Penn State University's Nobel Laureate Professor Alley (2018) was also asked about the issue. He said that energy unavailability created the problem. He did not know that India is running mad for energy productions, water acquisitions and reservations, and food productions. She provides free electricity and water to the farmers. Her food production got so much that huge surplus of grains rot in the storage facilities in northwest Punjab. On the face of hungry millions, India wasted both resources and energy. She wasted the water used in the production of food grains. Also, she wasted the energy required to move the water in irrigation. This is because massive energy is required in moving water in farming with the help of electric pumps. That makes the mine sector fall short of energy in lifting coal causing fuel shortages in running coal-fired power plants. A great discussion was held on "Choke Point: India initiative, an exploration into the water-energy-food confrontations in the world's second most populous country" on 2 April 2014

Figure 69. The main tributaries of the Indus that India and Pakistan receive according to the 1960-World Bank Mediated Indus Water Treaty
Source: SANDRP, 2017.

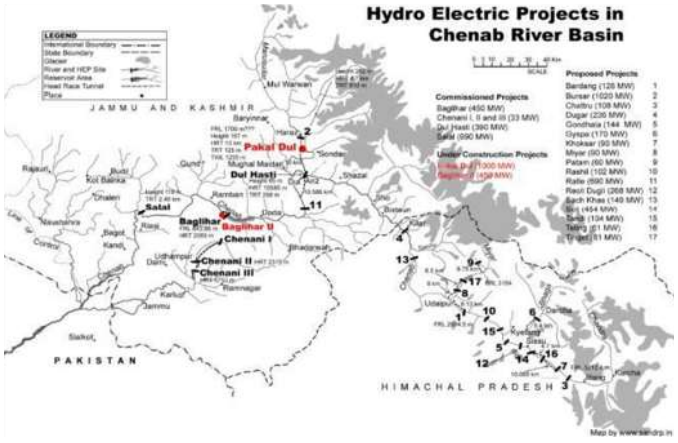

Figure 70. Hydroelectric projects in the Pakistan's shared Chenub River Basin that will affect the Indus discharge.
Source: SANDRP, 2017.

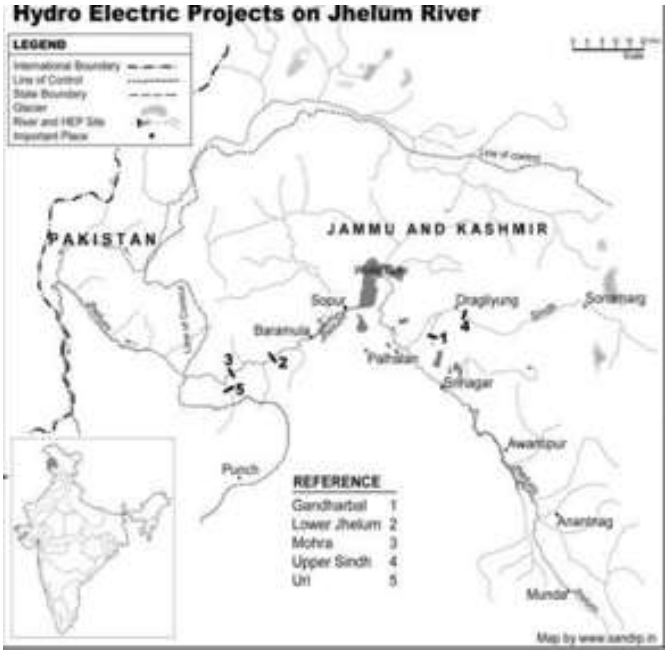

Figure 71. Hydroelectric projects on the Jhelum River
Source: SANDRP, 2017.

by the Circle of Blue and the Wilson Center (China Environment Forum Choke Point: India –A Wilson Center-Circle of Blue Joint Initiative, April 02, 2014//9; 00 am – 11:00 am). The Circle of Blue's initiative is very much informative and worth of taking lessons for India (https://www.wilsoncenter.org/event/choke-point-india-wilson-center-circle-blue-joint-initiative; Adel, 2015). We focus on curbing CO_2 production that is believed to cause warming. Before the CO_2 curbing race is over, inland surface water resources will be depleted. The problem can be solved easily if the upstream nations listen to what the Father of India said – "The world has enough resources to meet everybody's need but to no one's greed." Nations should focus on wind energy, solar energy, etc. instead of hydroelectricity.

Internationality of World Rivers

Worldwide there are 60, 53, 71, 39, and 38 international

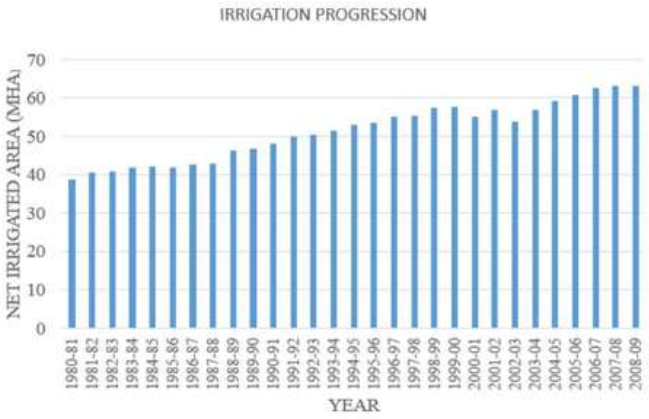

Figure 72. India's irrigation progression. (Plot made on the Statistics on Indian Economy and Society's data.
Source: https://www.indianstatistics.org/

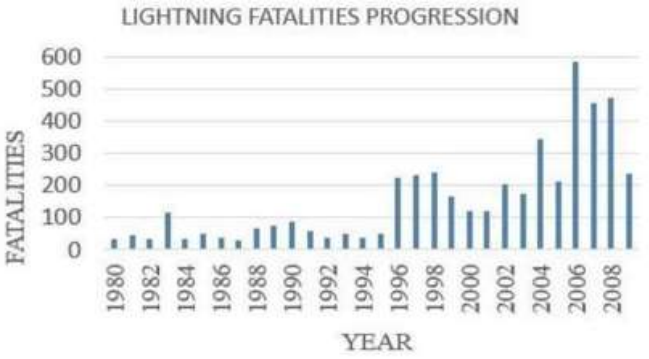

Figure 73. India's rising lightning fatalities.
Source: Singh and Singh (2015).

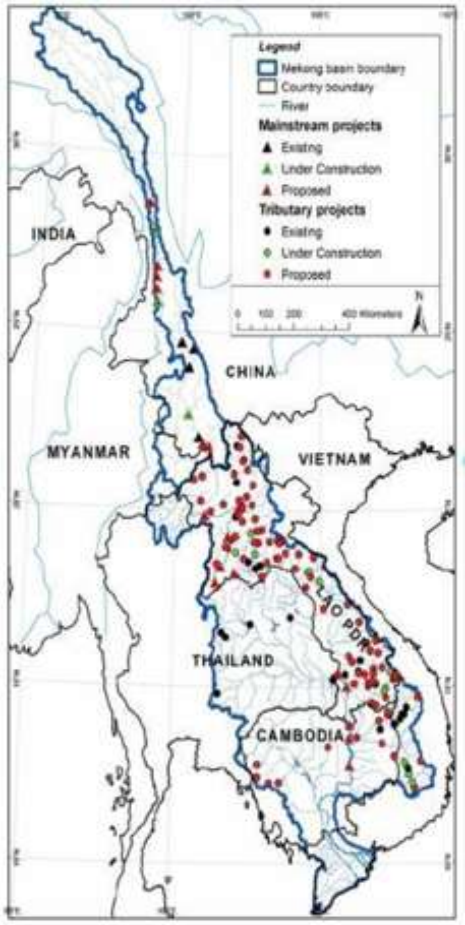

Figure 74. Shows the Mekong basin hydroelectric project sites including the operational, under-construction, and planned ones
Source: Houba et al. (2013)

rivers covering 62, 39, 54, 35, and 60% areas in Africa, Asia, Europe, North America, and South America, respectively. The percentages of international basin sharing by the number of countries are 90-100% by 39, 80-90% by 11, 70-80% by 14, 60-70 by 11, 50-60% by 17, 40-50 by 10, 30-40 by 10, 20-30% by 13, 10-20 by 9, and 0-10% by 1, respectively (Adel, 2015). Thus, the internationality of sweet water streams cannot be ignored for our mutual coexistence. If all other riparian countries follow the footsteps of India and China, a global havoc will be created. Covid-19 has targeted the global human population, but the upstream water piracy will affect all living beings – humans, animals, and the ecosystems. The best management of the international water resources is to use it by the upstream country as much as she needs and let remaining part flow downstream. The accumulation of excess water or rationing or blocking the downward flow is just piracy of water. It results in climate change both in the upstream (Adel, 2018) and in the downstream.

Table 5. Mekong basin planned and proposed dams.

Country	Planned	Proposed
Cambodia	12	0
China	11	2
Laos	43	20
Myanmar	7	0
Thailand	7	0
Vietnam	1	1
Totals	74	23

Source: Houba et al. (2013).

Conclusion

A pen picture of the Aral Sea basin-like scene, both existing and looming, along with warming vis-à-vis cooling

Figure 75. The Ganges's shrunken width ends as it falls in the Bangladesh territory
Source: Das, 2014.

has been presented. It should be an eye-opening for all of us to understand the importance of water in climate change. Water resources once gone are not recoverable due to its irreversibility. Its absence has a domino effect. As we live together, we should feel for each other. Motivation by self-interest mars others' interests, and even puts the self in jeopardy. Let there be a policy of current use of water and not storing for future. Let the water be released for the downstream after the need but not the greed of the upstream has served. Climatologists should not remain silent on the issue of hydroelectricity being used to corner a downstream neighbor, but instead focus on other forms of energy. If they can actively work on reducing CO2 emissions from industrialized nations, then they should not hesitate to speak out against the indiscriminate exploitation of water, the elixir of this living planet. CO_2 emission causes global warming, but the H_2O exploitation causes the dual effects of warming as well as cooling. A balanced amount of H_2O can protect the environment from extreme heating and cooling. Influential Nobel Laureate personalities like Professor Alley should understand the real picture and remove the wrong notion. As the pen is mightier than the sword, he should not be hesitant to speak the truth against any

nuclear power possessing nation.

CONFLICT OF INTERESTS

The author has not declared any conflict of interests.

ACKNOWLEDGEMENTS

The author is sincerely thankful to those individuals and agencies that have provided him with facts and figures to intellectually beautify the article.

REFERENCES

Adel MM (2002). Man-made climatic changes in the Ganges basin. International Journal of Climatology 22:993-1016.

Adel MM (2021). Physical Reasons for Increased Lightnings in Bangladesh and Mitigation Strategies. American Journal of Environmental Science (in review)

Adel MM (2013). Upstream water piracy contaminates downstream water. Environmental Justice 6(3):103-114.

Adel MM (2015). Farakka Barrage Vols 1& II: The Symbol of Bluffing, Blackmailing, Bullying, and Cornering Downstream for Upstream Water Piracy, published by German Academic Publishing Company Lap Lambert.

Adel MM (2018). The Uttarakhand 2013 and Jammu-Kashmir 2014 Disasters - Upstream effects of water piracy. African Journal of Environmental Science and Technology 12(1):21-68. basinhttp://sandrp.in/basin_maps/Hydropower_Projects_in_Brahmaputra_Basin.pdf

Adel MM, Hossain MR, Hossain SF (2014). Climatic severity victims of upstream water piracy strongly evidencing inland water depletion-caused global warming vis-a – vis cooling. American Journal of Environmental Science 10(2):171-198.

Anthony P (2006). Atlas of Asia. File: Location-Asia-UNsubregions.pn, retrieved from https://commons.wikimedia.org/wiki/File:Location-Asia-UNsubregions.png

Banglapedia (2021a). National Encyclopedia of Bangladesh. https://en.banglapedia.org/index.php/Ganges-Padma_River_System

Banglapedia (2021b). Irrigation. https://en.banglapedia.org/index.php/Irrigation

Banglapedia (2021c). Brahmaputra-Jamuna basin. https://en.banglapedia.org/index.php/Brahmaputra-Jamuna_River_System#:~:text=Brahmaputra%2DJamuna%20River%20System%20is,the%20largest%20floodplain%20of%20Bangladesh.

Beautiful Bangladesh (2012). Teesta Barrage. https://mybeautifulbangladesh.blogspot.com/2012/06/teestariver.html

BBC NEWS (2014). Megadams: Battle on the Brahmaputra https://www.bbc.com/news/world-asia-india-26663820.

Bosshard P (2011). People's Power Blocks Dam Construction in Northeast India, International Rivers. https://archive.internationalrivers.org/blogs/227/people%E2%80%99s-power-blocks-dam-construction-in-northeast-india

Das TK (2014). River Bank Erosion Induced Human Displacement and Its Consequences. https://www.researchgate.net/publication/279200603_River_Bank_Erosion_Induced_Human_Displacement_and_Its_Consequences/figures?lo=1.

Dey NC, Bala S K , Saiful Islam AKM, Rashid MA, Hossain M (2013). Northwest Bangladesh, BRAC. Available from http://www.nfpcsp.org/agridrupal/sites/default/files/ToR-2.pdf

Dolphin Conservation Committee of Kuakata, Bangladesh May 14, 2022. https://www.benarnews.org/english/news/bengali/dolphin-deaths-05272022135212.html

Drakopoulos PG, Ghionis G, Lazogiannis K, Poulos S (2014). Toward precise shoreline detection and extraction from remotely sensed images with the use of wet and dry sand spectral signatures. retrieved from https://www.researchgate.net/figure/Reflectance-spectra-of-different-sand-types-as-measured-in-the-laboratory-To-avoid_fig1_279316819

Dutta PK (2019). October 16, 2019 UPDATED: October 16, 2019 13:03 IS. T. PM Modi's water threat to Pakistan: What India can do under Indus Waters Treaty, India Today. Retrieved from https://www.indiatoday.in/india/story/pm-modi-s-water-threat-to-pakistan-what-india-can-do-under-indus-waters-treaty-1609883-2019-10-16

Food and Agriculture Organization of the United Nations (FAO) (2011). AQUASTAT Transboundary River Basins - Indus River Basin. FAO: Rome.

Google My Maps (2023). (https://www.google.com/maps/d/u/0/viewer?ie=UTF8&t=h&oe=UTF8&msa=0&mid=1S5JxMyEPrAS aD w jGZcr3h _ zh W 0&l l=2 4.8469 8912 49214 32% 2C 87.919 4521599 745& z =14

Hafiz M (2023). Global Water Crisis, Immineny Water War in Bangladeh perspective, the Daily Naydiganta, May 30 (in Bengali), https://www.dailynayadiganta.com/subeditorial/751847/%E0%A6%AC%E0%A7%88%E0%A6%B6%E0%A7%8D%E0%A6%AC%E0%A6%BF%E0%A6%95%E0%A6%AA%E0%A6%BE%E0%A6%A8%E0%A6%BF%E0%A6%B8%E0%A6%99%E0%A7%8D%E0%A6%95%E0%A6%9F%E0%A6%B8%E0%A6%AE%E0%A7%8D%E0%A6%AD%E0%A6%BE%E0%A6%AC%E0%A7%8D%E0%A6%AF%E0%A6%AA%E0%A6%BE%E0%A6%A8%E0%A6%BF%E0%A6%AF%E0%A7%81%E0%A6%A6%E0%A7%8D%E0%A6%A7%E0%A6%AA%E0%A7%8D%E0%A6%B0%E0%A7%87%E0%A6%95%E0%A7%8D%E0%A6%B7%E0%A6%BF%E0%A6%A4%E0%A6%AC%E0%A6%BE%E0%A6%82%E0%A6%B2%E0%A6%BE%E0%A6%A6%E0%A7%87%E0%A6%B6

Hebblethwaite G (1997). The impacts and implications of the Farakka barrage upon Bangladesh. (Doctoral dissertation, B. Sc. Thesis. Newcastle University. UK).

Hillary ES (1979). From Ocean to the Sky, Viking Publication, New York.

Hollander M, Wolfe D A (1999). Nonparametric Statistical Methods. John Wiley & Sons, Inc.: New York pp. 178-179.

Hoque KMR (2014). Sharp decrease of Jamuna water hampers navigation. The Daily Star, https://www.thedailystar.net/sharpdecrease- of-jamuna-water-hampers-navigation-51204

Houba H, Pham Do KH, Zhu X (2013). Saving a River: A Joint Management Approach to the Mekong River Basin. Environment and Development Economics 18(01):93-109.

https://m.somewhereinblog.net/mobile/blog/dhabian/30337144

https://m.somewhereinblog.net/mobile/blog/mostofa_kamal/30206906

https://www.thedailystar.net/teesta-to-affect-indo-bangla-relations-21336

Islam SN, Gnauck A (2011). Water Shortage In The Gorai River Basin And Damageof Mangrove Wetland Ecosystems In Sundarbans,Bangladesh, 3rd International Conference on Water and Flood Management (ICWFM-2011

Katz D (2008). EngineerRower in Bangladesh, February 14, 2008, available at http://donnybangla.blogspot.com/search/label/Rajshahi%20University Kondrtev IA (ed.). NASA: Springfield, VA; 580.

Magura Representative (2018). Four farmers died of lightning strikes. Published: 11 Sep 2018 05:39 PM BdST Updated: 11 Sep 2018 06:00 PM BdST (https://bangla.bdnews24.com/samagrabangladesh/article1538671.bdnews)

Map of India (2012). https://www.researchgate.net/publication/256038262_Technology_Spillover_of_Foreign_Direct_Investment_An_Analysis_of_Different_Clusters_in_India

Mazumder BS (1994). Grain size distribution in suspension from bed materials. Sedimentology 41(2):271-277.

McKinney DC (2003). 4th Draft (November 28, 2003), Cooperative Management of Transboundary Water Resources In Central Asia

from In the Tracks of Tamerlane-Central Asia's Path into the 21st Century, D. Burghart and T. Sabonis-Helf (eds.), National Defense University Press, 2003. (In press)
Micklin P (2007). The Aral Sea disaster. Annual Review of Earth and Planetary Sciences 35:47-72.
Mukherjee A, Bhanja SN, Wada Y (2018). Groundwater depletion causing reduction of baseflow triggering Ganges river summer drying. Scientific Reports 8(1):12049.
NASA Collage by Producer Cunningham (2014). A comparison of the Aral Sea in 1989 (left) and 2014 (right). Retrieved from https://commons.wikimedia.org/wiki/File:AralSea1989_2014.jpg
National Mission for Clean Ganga (NMCG). Course of Ganga https://nmcg.nic.in/courseofganga.aspx
Niyogi PK (2002). Nadia Rivers. File:Nadia Rivers.jpg, retrieved from https://commons.wikimedia.org/wiki/File:Nadia_Rivers.jpg
Niyogi PK (2008). Damodar basin. File:Damodar Map.jpg, retrieved from https://commons.wikimedia.org/wiki/File:Damodar_Map.jpg
Niyogi PK (1997). Main Rivers of North Bengal. File:BD Map Rivers of North Bengal2.jpg, retrieved from https://commons.wikimedia.org/wiki/File:BD_Map_Rivers_of_North_Bengal2.jpg
Ragab R, Prudhomme C (2002). SW—Soil and Water: Climate Change and Water Resources Management in Arid and Semi -arid Regions: Prospective and Challenges for the 21st Century, Biosystems Engineering 81(1):3-34.
Roy P (2014). Teesta river runs dry as India and Bangladesh fail to resolve disputes, The Third Pole, https://www.thethirdpole.net/en/regional -cooperation/teesta-riverruns-dry-as-india-and-bangladesh-fail-to-resolve-disputes/
Romps DM, Seeley JT, Vollaro D, Molinar J (2014). Projected increase in lightning strikes in the United States due to global warming. Science 346(6211):851-854.
SANDRP (2017). South Asia Network on Dams and Rivers, https://sandrp.in/2017/03/21/india-pakistan-resume-talks-on-industreaty-stakes-are-high/#
Sattar MA (1998). Bangladesh-Bharat Ovinno Nodir Pani Sankot (Bangladesh-India Transboundary River Crisis), Tofazzel Hossain Vishwya Sahitya Bhaban, Banglabajar, Dhaka, Bangladesh.
Sattar MA (1996). Farakka Bangladesher Bhagyo Zekhane Bondi, Padma-Jamuna Prakashani, Dhaka, Bangladesh.
Sinha D (2021). Meet the researcher trying to give Gangetic dolphins their due, Hindustan Times, https://www.hindustantimes.com/lifestyle/art-culture/meet-theresearcher-trying-to-give-gangetic-dolphins-their-due-101630101099743.html
Singh O, Singh J (2015). Lightning fatalities over India: 1979-2011. Meteorological Applications 22(4):770-778.
Sirajganj Representative (2018). Lightnings kill 10 buffalos. bdnews24.com.
Sufian SA (1993). Farakka Barrage- An Overview, in Proceedings of the International Seminar on Farakka Barrage, Farakka Committee (ed.), October 10, 1993, Columbia University, New York.
Thakkar H (2017). SANDRP, South Asia Network on Dams, Rivers, and People, Chenab · Indus · Pakistan India Pakistan Resume talks on Indus Treaty: Stakes are high. Retrieved from https://sandrp.in/2017/03/21/india-pakistan-resume-talks-on-indus-treaty-stakes-are-high/
The Daily Star (2014). http://news.bbc.co.uk/2/hi/south_asia/7192200.stm
The Daily Amar Desh. https://www.amardesh.com/
The Daily Janakantha (2020). https://www.dhakatribune.com/bangladesh/319168/teesta-flowing-above-danger-level-all-barrage
Thompson A (2014). Lightning May Increase with Global Warming, Scientific America, Climate Central on November 13. https://www.scientificamerican.com/article/lightning-may-increase-with-global-warming/
User Staecker (2003). Orphaned ship in former Aral Sea, near Aral, Kazakhstan. Retrieved from https://commons.wikimedia.org/wiki/File:Aralship2.jpg
Woo HS, Julien PY, Richardson EV (1988). Suspension of large concentration of sands. Journal of Hydraulic Engineering 114:888-898.
Zaman AN (2021). Boro paddy hit by heat wave. 10th April, 2021 11:39:33 AM in the Daily Sun retrieved from https://www.daily-sun.com/post/546343/Boro-paddy-hit-by-heat-wave
Zavialov P (2007). Physical Oceanography of the Dying Aral Sea Published by Springer Berlin Heidelberg, March 2007, DOI10.1007/b138791.

Related Journals: